

The Spite Lithium Plateau: Ultra-Thin but Post-Primordial¹

Sean G. Ryan

Royal Greenwich Observatory (closed), and Institute of Astronomy, Madingley Road,
Cambridge CB3 0HA, United Kingdom; email: sgr@ast.cam.ac.uk

John E. Norris

Research School of Astronomy and Astrophysics, The Australian National University,
Private Bag, Weston Creek Post Office, ACT 2611, Australia; email: jen@mso.anu.edu.au

and

Timothy C. Beers

Department of Physics and Astronomy, Michigan State University, East Lansing, MI
48824; beers@pa.msu.edu

Received _____; accepted _____

V1.0 for ApJ, 990301

¹Based on observations obtained with the University College London échelle spectrograph (UCLES) on the 3.9 m Anglo-Australian Telescope (AAT), the Double Beam Spectrograph (DBS) on the Australian National University 2.3m telescope, and the Utrecht échelle spectrograph (UES) on the 4.2 m William Herschel Telescope (WHT).

ABSTRACT

We have studied 23 very metal-poor field turnoff stars, specifically chosen to enable a precise measurement of the dispersion in the lithium abundance of the Spite Li plateau. We concentrated on stars having a narrow range of effective temperature and very low metallicities ($[\text{Fe}/\text{H}] \lesssim -2.5$) to reduce the effects of systematic errors, and have made particular efforts to minimise random errors in equivalent width and effective temperature. A typical formal error for our abundances is 0.033 dex (1σ), which represents a factor of two improvement on most previous studies.

One of the 23 stars, G186-26, was known already to be strongly Li depleted. Of the remaining 22 objects, 21 (i.e. 91% of the original sample) have abundances consistent with an *observed* spread about the Spite Li plateau of a mere 0.031 dex (1σ). As the formal errors are 0.033 dex, we conclude that the intrinsic spread σ_{int} is effectively zero at the very metal-poor halo turnoff. (Inclusion of the twenty-second star would inflate the observed spread to only 0.037 dex, leaving $\sigma_{\text{int}} < 0.02$.) Furthermore, we have established this at a much higher precision than previous studies (~ 0.06 – 0.08 dex).

Our sample does not exhibit a trend with effective temperature, though the temperature range is limited. However, for $-3.6 < [\text{Fe}/\text{H}] < -2.3$ we do recover a dependence on metallicity at $dA(\text{Li})/d[\text{Fe}/\text{H}] = 0.118 \pm 0.023(1\sigma)$ dex per dex, almost the same level as discussed previously. Earlier claims for a lack of dependence of $A(\text{Li})$ on abundance are shown to have arisen, in all likelihood, from the use of noisier estimates of effective temperatures and metallicities, which have erased the real trend. The dependence is concordant with theoretical predictions of Galactic chemical evolution (GCE) of Li (even in such metal-poor stars) and with the published level of ${}^6\text{Li}$ in two of the stars of

our sample, which we use to infer the GCE ${}^7\text{Li}$ contribution. The essentially zero intrinsic spread ($\sigma_{\text{int}} < 0.02$ dex) inferred for the sample leads to the conclusion that either these stars have all changed their surface Li abundances *very* uniformly, or else they exhibit close to the primordial abundance sought for its cosmological significance. Although we cannot rule out a uniform depletion mechanism, economy of hypothesis supports the latter interpretation. The lack of spread in the $A(\text{Li})$ abundances limits permissible depletion by current rotationally-induced mixing models to < 0.1 dex.

Correcting for the GCE contribution to both ${}^6\text{Li}$ and ${}^7\text{Li}$, we infer a primordial abundance $A(\text{Li})_p \simeq 2.00$ dex, with three systematic uncertainties of up to 0.1 dex each depending on uncertainties in the effective temperature scale, stellar atmosphere models, and correction for GCE. (The effective-temperature zeropoint was set by Magain’s and Bell & Oke’s $b - y$ calibrations of metal-poor stars, and the model atmospheres are Bell’s, without convective overshoot.) We predict that observations of Li in extremely low-metallicity stars, having $[\text{Fe}/\text{H}] < -3$, will yield smaller $A(\text{Li})$ values than the bulk of stars in this sample, consistent with a low primordial abundance.

The difference between our field star observations and the M92 data in the literature suggests that real field-to-cluster differences in Li evolution may have occurred. This may indicate different angular momentum evolutionary histories, with interactions between protostellar disks in the dense globular cluster environments possibly being responsible. Further study of Li in globular clusters and in very metal-poor field samples is required to clarify the situation.

Subject headings: early Universe — cosmology: observations — nuclear reactions, nucleosynthesis, abundances — stars: abundances — stars: Population II — Galaxy: halo

1. Introduction

Beginning with Spite & Spite (1982), many authors have used the apparent uniformity of the abundance of lithium in the atmospheres of metal-poor ($[\text{Fe}/\text{H}] < -1.0$) subdwarfs warmer than $T_{\text{eff}} = 5600$ K to infer the primordial value generated by standard Big Bang nucleosynthesis. By restricting a sample to $T_{\text{eff}} > 5600$ K, one avoids well-documented processes which alter the surface Li abundance in cooler dwarf stars (e.g. Deliyannis, Demarque, & Kawaler 1990). If this interpretation is correct, the so-called “Spite Li Plateau” abundance of $A(\text{Li}) = 12 + \lg(N(\text{Li})/N(\text{H})) \simeq 2.1$ provides constraints on the baryon-to-photon ratio in the early universe, and hence Ω_b (e.g. Deliyannis 1995)².

However, several theoretical and observational results have cast doubt on use of the observed Li plateau abundance as the primordial value. Lithium is fragile, and some stellar evolutionary models show that Li could have been depleted by an order of magnitude from a high primordial value and still attained plateau-like abundances by the age of the halo (e.g. Pinsonneault, Deliyannis, & Demarque 1992). More recent computations by Pinsonneault et al. (1998), using an improved treatment of angular momentum evolution and comparisons with more modern observations, have reduced the permissible ${}^7\text{Li}$ depletion to the range 0.2–0.4 dex. Trends of lithium abundance with T_{eff} and $[\text{Fe}/\text{H}]$ (effectively a tilted plateau) have also been measured (Thorburn 1994; Norris, Ryan, & Stringfellow 1994; Ryan et al. 1996a) which would not exist if the Li were primordial, though these results may be driven by larger than expected systematic errors in the effective temperatures (Bonifacio & Molaro 1997). The huge (> 1 dex) Li deficiencies in some stars which are otherwise indistinguishable from normal plateau stars (Hobbs, Welty, & Thorburn 1991; Thorburn 1994; Norris et al. 1997a; Ryan, Norris, & Beers 1998) highlight the incompleteness of our

² $\lg X = \log_{10} X$

understanding of Li processing in halo stars.

A direct challenge to the thesis of a primordial, and therefore uniform, Li plateau was mounted by Deliyannis, Pinsonneault, & Duncan (1993), and supported by Thorburn (1994), who argued that the spread in measured plateau-star abundances exceeds that expected from observational errors. Deliyannis et al. tabulated a range of dispersions, depending on the characteristics of the sample, but with a *minimum* spread of $\sigma = 0.04$ dex, while Thorburn (1994) found a value around 0.1 dex for a much larger sample. Both groups concluded that Li production and/or depletion mechanisms had operated prior to the birth or during the evolution of the stars, in which case the measured Li abundance would not reflect solely that from Big Bang nucleosynthesis. Large ranges in Li abundance have also been deduced for subgiants in M92 (Deliyannis, Boesgaard, & King 1995; Boesgaard et al. 1998). As further evidence of star-to-star differences in the halo field, Ryan et al. (1996a) cited the three stars G64-12, G64-37, and CD-33°1173, all of which have extremely low metallicities ($[\text{Fe}/\text{H}] < -3$), are apparent non-binaries, and have surface temperatures $T_{\text{eff}} \approx 6250$ K, but for which they computed abundances $A(\text{Li}) = 2.29 \pm 0.05$, 2.01 ± 0.04 , and 1.89 ± 0.06 , respectively.

However, the case for a measurable dispersion in the Li plateau has not gone unchallenged. Most recently, Molaro, Primas, & Bonifacio (1995), Spite et al. (1996), and Bonifacio & Molaro (1997) have questioned whether some of the error estimates in earlier works were realistic, and have suggested that the dispersion is no greater than 0.08–0.10 dex, less than that found by Thorburn (1994), but not excluding the smaller scatter of Deliyannis et al. (1993). Ryan et al. (1996a) noted that most, but not all, published measurements could be reconciled within their claimed errors, thus illustrating that some error estimates were optimistic, a result which biases one towards over-interpreting the spread about the mean plateau value.

We set out to provide a substantially more accurate assessment of scatter about the Li plateau, to see whether we could rule out a purely primordial interpretation, or whether the width was essentially consistent with small uncertainties in the measurements and analysis. We note at the outset that a very thin plateau is a necessary but not sufficient condition for the observed abundance to be primordial. The Li plateau may be of infinitesimal width, but depend on effective temperature and/or metallicity, in which case it will still not provide the primordial abundance, though some stars may be very close to it.

2. Definition of the Sample

We sought very high signal-to-noise (S/N) measurements of the 6707 Å Li doublet in a group of well-selected halo stars, with the aim of measuring Li abundances to higher precision than had been routinely accomplished previously.

Estimates of the effective temperatures of stars are notoriously uncertain, particularly absolute as opposed to relative estimates, yet derived Li abundances depend on temperature. For example, the existence of temperature-dependent trends in the Li plateau depends on which effective temperature scale is adopted (compare Ryan et al. (1996a) and Bonifacio & Molaro (1997)). Uncertainties in star to star abundance comparisons also increase if their temperatures differ, because stellar atmosphere structures and color-effective temperature transformations also depend on temperature. To minimise the effects of systematic errors, we restricted our sample to a very narrow range in T_{eff} , and chose a narrow metallicity regime ($[\text{Fe}/\text{H}] \lesssim -2.5$), since this avoids possible metallicity-dependent errors in the color-effective temperature transformation and model stellar atmospheres. Our sample targeted effective temperatures in the range $6100\text{K} (\pm 50) < T_{\text{eff}} < 6300\text{K} (\pm 50)$, metallicity in the range $-3.5 \leq [\text{Fe}/\text{H}] \leq -2.5$. We also restricted our sample to stars brighter than $V = 13$ because of the requirement for high S/N.

The narrow temperature range places the stars at the turnoff of an old main-sequence population, effectively eliminating subgiants which spent their main-sequence lives at higher temperatures than those now observed, and hence have different evolutionary histories. Another benefit of this restriction is that the surface gravity of the sample covers only a narrow range at the turnoff, though it has been noted many times previously that the Li abundance derived for halo dwarfs is quite insensitive to surface gravity errors. The use of very low metallicity stars means that we are sampling material which has undergone a minimum of nucleosynthetic processing since the Big Bang.

We developed a target list of approximately 30 stars from the surveys of Schuster & Nissen (1988), Ryan (1989), Beers, Preston, & Shectman (1992), and Carney et al. (1994). A large sample was sought to reduce the impact of one or two “pathological” objects, such as marginally depleted examples of the ultra-Li-depleted stars or unrecognised binaries. We hoped to make multiple measurements of each one to verify the repeatability and to provide a check for radial velocity variability.

With the available telescope time, 22 of the stars were observed, and these are presented in Table 1. Also included in the table is G186-26, a known ultra-Li-depleted star (Hobbs, Welty, & Thorburn 1991) which satisfied our selection criteria, but which we chose not to reobserve since its surface Li deficiency is already well established. Its relevance to our work is as a reminder that at least some otherwise similar stars have depleted the vast majority of their Li.

3. Basic Data

The stars have Johnson-Cousins photometry from a small number of sources referenced in Table 1, whose consistency and accuracy have already been established at $\sigma = 0.010$ mag

per observation for B–V and R–I, and $\sigma = 0.007$ mag in V–R (Ryan 1989). Strömgren photometry from Schuster, Nissen, and collaborators (see references in table) is available for all but one star. The columns headed n_J , n_S , and n_β in the table give the number of BVRI, uvby, and β measurements respectively. Multiple measurements improve the photometric accuracy, which is important in deriving effective temperatures for the stars. We reduce the Johnson errors to 0.007 (for B–V and R–I) and 0.005 (for V–R) for two or more observations. Where rounding errors of up to 0.005 mag affect Johnson-Cousins colors quoted to only 0.01 mag, we adopt larger uncertainties — 0.015 (for B–V and R–I) and 0.010 (for V–R) for single measurements, and 0.010 (for B–V and R–I) and 0.007 (for V–R) for two or more measurements. Schuster & Nissen (1988) quote mean errors less than 0.008 mag for $b - y$ and 0.011 mag for β where there are three observations per star. Given that all of our program stars have 3 or more Strömgren observations, we adopt these error estimates for our entire sample.

Estimates of the interstellar reddening have been obtained from two techniques. Values estimated from reddening maps (Lucke 1978; Burstein & Heiles 1982) and Johnson photometric distances have been made by Carney et al. (1994) and Ryan (1989), and are listed in Table 1 as $E(BV)$. Strömgren photometry estimates of $E(b - y)$ are based on a comparison of the $b - y$ color and β reddening-free index (Schuster & Nissen 1989, eq. (1)), and these values are tabulated under $E(by)$. Based on the central wavelengths of the bandpasses and a $1/\lambda$ reddening law, a relation $E(b - y) = 0.7 \times E(B - V)$ is expected. However, comparison of the $E(B - V)$ inferred from the Strömgren values with the map-based values shows that the former are higher by 0.020 mag. The Strömgren technique suggests a mean reddening for the sample of $\langle E(B - V) \rangle = 0.035$ mag, whereas the map-based values suggest $\langle E(B - V) \rangle = 0.015$ mag. We lack solid evidence as to which reddening scale — map or Strömgren — is better, but as the sample is fairly bright, we expect the intrinsic reddening to be low, so reduce all Strömgren values of $E(B - V)$ by 0.020 mag prior

to averaging³. Once this offset is taken into account, the RMS error inferred for a single $E(B-V)$ estimate is 0.009 mag. This error is assumed to affect all dereddening vectors of non-zero magnitude. We adopt $E(V-R) = 0.78 \times E(B-V)$ and $E(R-I) = 0.82 \times E(B-V)$ following Savage & Mathis (1979).

Table 1 also records measurements of the $H\delta$ line spectroscopic index, $HP2$, from Beers et al. (1999) supplemented with new, 1Å-resolution, high S/N determinations based on observations with the 2.3m telescope on Siding Spring Mountain in 1998 March and September. This pseudo-equivalent width index complements the β index and helps establish the effective temperature scale (below). It has the benefit of being independent of reddening, essentially independent of metallicity for our metal-poor sample, and having better temperature sensitivity than β for the temperatures of our sample.

4. Spectroscopic Observations and Data Reduction

4.1. Observational Program

Previous investigations of the Li plateau (see §1) claimed the significance of spreads at levels $\sigma \sim 0.08\text{--}0.10$ dex, but Deliyannis et al. (1993) showed that the Li spread could be as small as $\sigma = 0.04$ dex, depending on which subsample of stars they analysed. These values indicated that we would require accuracies of order $\leq 10\%$, or ≤ 0.04 dex, to clarify the situation. The equivalent width for the Li line in halo turnoff stars is ~ 20 mÅ, thus requiring $\sigma_W \lesssim 2$ mÅ. This in turn demanded high resolution spectra ($R \sim 40000$, which

³We cannot discount the possibility that the Galaxy does indeed have a high local reddening. This has been suggested already by Schuster et al. (1996) who find, on the basis of Strömgren photometry, an average reddening of 0.036 within 30° of the South Galactic Pole.

just resolves the 6707 Å Li doublet) and high S/N.

Observations were made using the University College London échelle spectrograph (UCLES) at the coudé focus of the Anglo-Australian Telescope, spread over four epochs (in many instances utilising partial nights). Two different observers acquired the data as follows: August 28, 1996 (SGR); August 18–23, 1997 (JEN); April 8–10, 1998 (JEN); and August 10–15, 1998 (SGR). Although cross-dispersed échelle spectra often have only limited spatial coverage which makes the sky and scattered light level difficult to measure, we used UCLES with its 79 lines mm^{-1} grating, which gives a 14 arcsec slit length, thus providing an unambiguous background subtraction. The spectra are shown co-added for multiple epochs in Fig. 1. For the northern star BD+9°2190, we had only one low S/N ($=85$) measurement with the AAT, so we obtained a supplementary observation in service time with the Utrecht échelle spectrograph (UES) at the Nasmyth focus of the William Herschel Telescope, on November 5, 1998. The UES is almost identical to the UCLES.

The Li measurements (discussed in detail in §4.2) are presented in Table 2, where we tabulate for each epoch: the S/N, the equivalent width, and the equivalent width error. The S/N is taken as the lesser of that expected from Poisson photon statistics and the scatter actually measured about the continuum fit. The variance $^{-1}$ -weighted sum, \bar{W} , and error $\sigma_{\bar{W}}$, are also provided, as are two [Fe/H] values and our estimates of the effective temperature (see §5). The first column of [Fe/H] values is from the literature and derives from high- and/or medium-resolution spectroscopic observations, for which the errors are believed to be $\sigma \simeq 0.15$ dex (see references in table). The second [Fe/H] entries were obtained by applying the calibration of Beers et al. (1999) to the 1 Å-resolution spectra from which the HP2 index was measured. The agreement between the two sets of values is very good; we shall return to this point later in the discussion.

To obtain the precision needed to examine potentially small levels of scatter about

the Spite Li plateau, it was clear that we would need very accurate equivalent width measurements. In an earlier work (Norris et al. 1994) we estimated our Li equivalent width uncertainties due to random noise as $\sigma(W) = 150/(S/N_{50})$ mÅ, where the S/N was per 50 mÅ pixel. In the current study we sum over a wider band to be more certain of including all of the line (see below), and so derive a larger numerator giving $\sigma(W) = 184/(S/N_{50})$ mÅ. As most epochs (except the single-night pilot run in 1996) have S/N in excess of 100, we expected to achieve accuracies better than 2.0 mÅ per observation.

High absolute accuracy is harder to achieve than high internal precision. We discuss internal and external errors below, emphasising that our primary requirement in studying scatter about the Li plateau is a large, homogeneously selected, consistently reduced, precisely measured, and consistently analysed set of data. Several procedures were adopted to identify and minimise errors in order to meet this requirement. Firstly, we sought two epochs of data on each star to permit us to verify the repeatability of each measurement; we obtained multiple observations for 12 of the 22 stars. Secondly, all raw data were reduced by two of us independently, using different software. This allowed us to verify that the reduced spectra were consistent irrespective of which software, algorithms, and personal techniques were applied. Finally, two different techniques were used to measure the equivalent widths from the reduced spectra.

4.2. Details on Equivalent Width Measurements

4.2.1. Continuum Placement

The spectra of very metal-poor main-sequence-turnoff stars are essentially devoid of lines over the range 6700–6715 Å apart from the 6707 Å Li doublet itself. Even the Ca I line at 6717 Å is invisible at the low metallicity and warm temperatures of many of these

objects. (An equivalent width $W_{6717} < 1$ mÅ is expected for a model with $T_{\text{eff}} = 6000$ K, $\lg g = 4.0$, and $[\text{Fe}/\text{H}] = -3$.) The continuum can therefore be defined accurately and objectively by fitting the mean flux on either side of the Li doublet. Two techniques for measuring equivalent widths are described in the following subsection. For the direct summation method, the continuum was computed as a quadratic fit to the flux in zones 2.5 Å wide on either side of a 1.2 Å-wide zone of avoidance centred on the Li feature. The Gaussian-fitting technique employed a linear continuum, again using the mean flux on either side of the Li feature, though the exact width of each continuum zone (approx. 4 Å) was allowed to vary from star to star.

4.2.2. *Equivalent Width Calculations*

The Li 6707 Å doublet separation is quite large (0.15 Å), so for the narrow range of line strengths in our program stars, the FWHM of the spectral feature is not very sensitive to the instrumental resolution, which was in any event constant throughout the observing program. We also confirmed that the line broadening of the Mg 'b' lines was similar in all objects, as a check against rotational broadening or the presence of a barely-resolved spectrum of a secondary companion. As a result of the similarity of our program stars, the actual width of the doublet line is expected to be constant for all of them, with only the line depth responding to equivalent width differences.

Once the continuum was defined, equivalent width measurements were made in two ways.

The first measurement technique was to centroid on the Li doublet, and then compute the equivalent width from the residual flux summed within a band ± 0.34 Å of that centroid. The width of this band was set considering the known width of the doublet and resolving

power of the spectrograph, and confirming on the spectra that this was a sensible choice. The very high S/N observations of HD 140283, whose Li equivalent width (48 mÅ) is larger than the program stars and thus sets an upper limit on the FWHM of the doublet in our (hotter) stars, showed that <1% of the absorbed flux would be missed over a band width of ± 0.34 Å. At the same time we avoid unwanted sensitivity to noise fluctuations that would arise if we summed over more pixels than necessary.

The second technique involved performing a Gaussian fit, but with the Gaussian FWHM fixed at 0.305 Å, again determined from the HD 140283 observations. As noted above, since the Li line is weak and the doublet resolved, its FWHM is determined by the doublet separation and the instrumental profile rather than the equivalent width. This procedure was adopted to avoid having noise in the line cause unphysical line widths in the fit.

Measurement of a given spectrum with the two equivalent width techniques (direct summation and constrained Gaussian fitting) showed good agreement. For the 1997 data, the mean difference between measurements and its standard deviation was $\langle W_{\text{sum}} - W_{\text{Gauss}} \rangle = -0.3$ mÅ, with $\sigma = 1.7$ mÅ. Similarly, for the 1996 data, the mean difference was $\langle W_{\text{sum}} - W_{\text{Gauss}} \rangle = -0.1$ mÅ, with $\sigma = 1.8$ mÅ. This gives us confidence that the two techniques introduce no significant systematic differences. (This test was not repeated in 1998, as there had been no changes to the procedures.)

As noted above, two authors reduced the data independently. Once we were satisfied that both equivalent width measurement techniques gave consistent results, one approach was applied by one author to his spectral reductions, and the second technique was applied by the other. The average of the two measurements was then adopted for each epoch.

4.2.3. Internal Errors

Our error estimates are based on the random noise accumulated over the width of the line (e.g. Cayrel 1988). For our pixel spacing and the width over which we measure the line in the direct summation method, we obtain the relationship $\sigma(W) = 184/(S/N_{50})$ mÅ where S/N_{50} is for a 50 mÅ pixel. Before utilising this model in the abundance analysis, however, we made three checks for consistency.

The first test assesses whether different authors using different data reduction algorithms and software generated mutually consistent reduced spectra. The differences of equivalent widths measured by a given technique for author A's and author B's spectra were $\langle W_A - W_B \rangle = +0.4$ mÅ, with $\sigma = 1.3$ mÅ for the 1997 data, and $\langle W_A - W_B \rangle = -0.3$ mÅ, with $\sigma = 2.6$ mÅ for the 1996 data. The systematic differences are negligible and the standard deviations acceptable, being comparable with the expected noise. (The test sequence was not repeated with 1998 data.)

The second comparison investigates whether the net effect of using separate reduction routes and two distinct measurement techniques is consistent with the noise model. The error distribution inferred from the difference between each pair of measurements should be *narrower* than that based on photon noise, since the techniques differ in the way they measure a noisy spectrum, but sample the *same* data and thus are exposed to the *same* noise. The measurement pairs can therefore be inspected to see whether they provide evidence that the random noise model is optimistic. The null hypothesis is that the error distribution inferred from the measurement pairs is not wider than that calculated from the model. The error distribution of each pair of measurements was estimated as the sample standard deviation $s_w = \frac{1}{\sqrt{2}}|W_{\text{Gauss}} - W_{\text{sum}}|$, and a standardised statistic Z_{pair} was computed by dividing by the model error, σ_W . Only seven of the forty pairs have Z_{pair} values exceeding 1.0, the maximum value being 1.8, so the null hypothesis could not be

rejected. That is, we sought and failed to find evidence that the noise model is optimistic and should not be trusted.

The third test was to compare equivalent widths we measured from spectra obtained on more than one epoch, to check for repeatability. We began by computing the variance⁻¹-weighted mean equivalent width for each star, \bar{W} , and the variance of the weighted mean, $\sigma_{\bar{W}}$ (e.g. Bevington 1969). These values are given in Table 2. Next, we computed the standardised residual, Z , for each observation as $Z = (W - \bar{W})/\sigma_{\bar{W}}$. The Z distribution has a standard deviation of 1.0 (or 1.1 if restricted to stars with three observations), standardised residual with the largest magnitude is +2.1, which shows that all but one of the thirty values falls within ± 2 standard deviations of the mean. In other words, the repeatability achieved from run to run is again consistent with the noise model.

4.2.4. External Errors

Although it is internal consistency which is most important for this study, it is nevertheless valuable to know whether or not our data are consistent with the work of others.⁴ Norris et al. (1994) and Ryan (1995) highlighted differences between Li equivalent width measurements for LP 815-43, which ranged over a factor of two from 13 ± 2 mÅ and 15 ± 3 mÅ (Norris et al. 1994) to 22 ± 2.1 mÅ (Thorburn 1994) and $27 \pm (3-6)$ mÅ (Spite & Spite 1993). Our new measurement, 16.1 ± 1.6 mÅ, is consistent with our earlier measurements, and reemphasises the importance of homogeneity in obtaining small *random* errors. It is the development of a large *homogeneous* data set in the current work which has allowed us to probe the scatter about the Li plateau with a much higher precision than

⁴We elected not to risk decreasing the homogeneity of the data set by combining it with other studies from the literature, including our own earlier work.

previous work, typically conducted at the 0.06–0.10 dex level.

Most studies in which new Li data have been presented have analysed only a dozen or so stars, so it is difficult to establish what, if any, systematic differences exist for the various studies, as the systematics can differ from one study to the next. Ryan et al. (1996a) addressed this issue using the extensive data set of Thorburn (1994) as a baseline for comparison, but found “either there were too few stars for a reliable comparison, or else the differences that existed could not confidently be ascribed to systematic errors amenable to transformation” onto a unified system. The one exception was a small but clearly systematic offset (3 mÅ) for the Thorburn vs Spite & Spite (1993) samples.

In Table 3 we present previous Li equivalent width measurements of our program stars and the three “standard” stars. Perusal of the list shows no cause for alarm that our data are systematically different from our previous work or that of others, except perhaps for the Spite & Spite (1993) sample as discussed above. The most precise observations in the table are the high S/N, high resolving power data obtained by Smith, Lambert, & Nissen (1998) (using different facilities to us) to measure the ${}^6\text{Li}/{}^7\text{Li}$ isotope ratio. We plot our measurements against theirs in Fig. 2. For the five stars in common, two agree within 1σ . and the remaining three agree within $1.2\text{--}1.8\sigma$. This comparison leaves us confident that, even though it is the high internal precision that is required for this study, our equivalent width measurements are also of high absolute accuracy.

4.3. Radial Velocity Measurements

To provide a check on unrecognized binarity among our program stars, we have also measured precise radial velocities. Although there are few spectral lines near Li 6707, the échelle spectra extend sufficiently blueward to include the Mg ‘b’ triplet and neighboring

lines. The spectra were cross-correlated over the wavelength region 5160–5200 Å, using the 1997 observation of HD 140283 as the template. The zeropoint velocity was then set by measurements of 42 apparently unblended lines in that spectrum, which gave a formal error of ± 0.1 km s $^{-1}$ (1 s.e.).

The heliocentric radial velocity for each epoch is given in Table 4, along with measurements from Carney et al. (1994 — CLLA94 in the table). The “Notes” column gives, for the Carney et al. entries, the dispersion (1σ) of their velocity measurements, the number of observations made, and the span (in days) of their series of observations. Excluding the previously known single-lined spectroscopic binary (SB1) — BD+20°2030 — and one clear new detection in this work, CD−71°1234, the typical scatter for our multiple measurements and for the difference between our measurements and those of Carney et al. is 0.3 km s $^{-1}$ (1σ). This is consistent with the external accuracy we have obtained previously with similar observational material (Norris, Ryan, & Beers 1997). There is no overwhelming evidence for binarity in the other stars at this level of accuracy; unrecognised binaries must have very low velocity amplitudes and/or very long periods which, statistically at least, suggests that their companions will have minimal impact on our analysis. Consequently, we may infer that the impact of unrecognised binarity is minor.

5. Effective Temperatures

5.1. Observational Indices

Deliyannis et al. (1993) attempted to circumvent the uncertainties in color-temperature transformations by working with color alone. However, it is implicit in such a procedure that the color, along with its random errors, accurately ranks the stars over the full range of the sample. We have taken a different approach to minimise the effects of errors, that of

restricting the diversity of stellar types at sample selection. The dereddened c_1^0 vs $(b - y)_0$ diagram (Fig. 3) confirms that the stars are within 0.05 mag in $b - y$ of the Population II main sequence turnoff. Nevertheless, to reach the desired level of accuracy we need to resolve even small temperature differences between almost identical stars, and hence fully utilise the available temperature indices (e.g. Spite et al. 1996). We can improve on the studies that adopt only a single color by having up to six indices ($b - y$, B–V, V–R, R–I, β , and HP2) on which to base effective temperatures; these are shown in Fig. 4 as a function of $(b - y)_0$.

Several color-effective temperature scales from the literature are also shown in Fig. 4. Panel (a) shows the B–V vs $b - y$ theoretical colors of Bell & Oke (1986) for $[\text{Fe}/\text{H}] = -2$ and $\lg g = 4.0$, which coincide roughly with the data, and the transformation of Magain (1987, eq(15) & (16)) at $[\text{Fe}/\text{H}] = -2.8$ (the mean metallicity of our sample) which sits away from the data, showing that Magain’s B–V and $b - y$ scales are not mutually consistent for these stars. Magain’s and Bell & Oke’s $b - y$ scales are almost identical for metal-poor turnoff stars, Bell & Oke’s scale being hotter by 7 K at 6100 K and 22 K at 6300 K. The Bell & Oke (V–R)_C and (R–I)_C colors are shown in Figs 4(b) and 4(c).

Panels (d) and (e) show the good correlation between $(b - y)_0$ and the Balmer line indices, β and especially HP2. A least-squares fit to the data permits estimates of the $(b - y)_0$ colors from the observed Balmer indices, which we call $(b - y)_\beta$ and $(b - y)_{\text{HP2}}$.

5.2. Calibrations

As our sample spans a 1 dex range in metallicity, it is important to understand the sensitivity of the effective temperature indicators to $[\text{Fe}/\text{H}]$. In very metal-poor turnoff stars, we do not expect the chosen indices to be sensitive to abundance. We sought to

verify this through available effective temperature calibrations, and especially to check the sensitivity of B–V since this index was expected to have the greatest dependence, if any.

According to Magain's (1987) B–V empirical calibration, which is based on 11 stars with $[\text{Fe}/\text{H}] < -1$ and temperatures derived from the infra-red flux method (IRFM), changing $[\text{Fe}/\text{H}]$ from -2.5 to -3.5 would change the inferred T_{eff} of turnoff stars by less than 1 K. However, the small size of this figure may be driven by the analytical form of Magain's fitting function, which is linear in metallicity (Z/Z_{\odot}) and hence loses sensitivity to this variable at even moderate metal deficiency. It also should be borne in mind that the most metal-poor member of Magain's calibration set was HD 140283, for which $[\text{Fe}/\text{H}] = -2.6$ (Ryan, Norris, & Beers 1996b), at the upper end of the present sample's metallicity range.

One recent and extensive calibration is the table of synthetic colors computed by Kurucz (1993) for a comprehensive range of observable indices, tracing metallicity sensitivity down to $[\text{Fe}/\text{H}] = -5$. Gratton, Carretta, & Castelli (1996) have shown that zeropoint differences are still found with other calibrations, but they nevertheless adopted the Kurucz metallicity dependence in devising their own transformation. This metallicity dependence is shown in Fig. 5(a)-(e) (*solid curves*) for pairs of colors typical of metal-poor turnoff stars. Magain's B–V and $b - y$ calibrations are also shown (*dashed curves*).

A more recent empirical calibration is that by Alonso, Arribas, & Martinez-Roger (1996a), which uses the large calibrating set of IRFM temperatures of Alonso, Arribas, & Martinez-Roger (1996b). They give fitting functions for a wide range of stellar types, but unfortunately these become non-physical for turnoff stars below $[\text{Fe}/\text{H}] \sim -2.5$. Figure 5(a) (dotted curves) shows the run of T_{eff} as a function of $[\text{Fe}/\text{H}]$ for a pair of B–V colors (0.35 and 0.40) appropriate to turnoff stars. Although the curves exhibit a reduction in sensitivity to metal abundance as $[\text{Fe}/\text{H}]$ falls from -1.0 to -2.6 , the fitting function goes

through a minimum and climbs again at lower metallicity. It is unreasonable to expect that stars of yet lower $[\text{Fe}/\text{H}]$ exhibit *stronger* sensitivity to metallicity, and such behavior is not supported by the Kurucz colors. Clearly this behavior reflects the form of the fitting function and the values of the coefficients, rather than the characteristics of metal-poor turnoff stars. (Alonso et al.’s fitting functions have a quadratic form so do not have the monotonically decreasing property of Magain’s.) Although Alonso et al.’s B–V calibration may be an improvement for the majority of stars, it is not applicable to our very metal-poor sample. Similar results obtain for most other indices in Alonso et al.’s calibrations. Figures 5(b)–(e) show that the V–R, $b - y$, and β calibrations also show non-physical forms at very low metallicity, $b - y$ being the most dramatic. We have to disagree with Alonso et al. that their transformation equations are valid down to $[\text{Fe}/\text{H}] = -3.5$. The most we can infer is that the metallicity sensitivity appears to saturate (reaches a minimum) by the time $[\text{Fe}/\text{H}]$ falls to -2.5 , and for some indices saturates at considerably higher $[\text{Fe}/\text{H}]$.

The metallicity range of our sample is indicated by a solid bar in Fig. 5(a). What is important for the present study is that *over the metallicity range of our sample, $-3.5 \leq [\text{Fe}/\text{H}] \leq -2.3$, all of the effective temperature indices we have used should possess essentially zero sensitivity to metallicity*. In Kurucz’s calibration, which is the only one of the three sensitive over our abundance regime, no index demonstrates a change by more than 18 K over the interval from $-3.5 \leq [\text{Fe}/\text{H}] \leq -2.5$. We thus feel justified in assuming that there is no significant metallicity dependence in any of our photometric indices.

We note for completeness that we inspected the data for any metallicity dependence in the difference between the dereddened B–V color and that predicted from $b - y$ by Bell & Oke’s B–V vs $b - y$ calibration. No significant dependence was found.

5.3. Combining Indices

We calculated temperatures for each of the indices shown, following Magain and Bell & Oke in adopting linear relationships between T_{eff} and color over the short temperature range involved, and adopting zero sensitivity to metallicity due to the considerable metal-deficiency of our sample. Minor extrapolation was required to use the Bell & Oke calibrations for stars hotter than 6250 K.

Temperature scales from different indices are seldom in agreement. We went through the exercise of computing linear transformations between the different temperature scales, but given the short temperature baseline covered by our stars we doubted the reliability of the scale factors (slope coefficients), and have instead applied zeropoint adjustments only. We use Magain's $b - y$ scale as the zeropoint (which essentially matches Bell & Oke's $b - y$ scale), and offset the Bell & Oke-scale temperatures as follows: $T(V-R) = T(V-R)_{\text{BO}} - 165$ K; $T(R-I) = T(R-I)_{\text{BO}} - 155$ K; and $T(B-V) = T(B-V)_{\text{BO}} - 85$ K. We also computed a temperature (on Magain's scale) based on the estimates $(b - y)_{\beta}$ and $(b - y)_{\text{HP2}}$.

The adopted effective temperature for each star is the variance⁻¹-weighted mean of the $b - y$, $(b - y)_{\beta}$, $(b - y)_{\text{HP2}}$, and re-based B-V, V-R, and R-I temperatures, using the variances for the individual temperature estimates determined from the photometric errors. The error estimates in temperatures derived from the β and HP2 indices include both the uncertainty in the measurement of each spectral index itself and the uncertainty in the $(b - y)_0$ value that is inferred from the least-squares fit (Fig. 4(d) and (e)). Temperatures and uncertainties are given in Table 2 (to the nearest 10 K). Temperatures from B-V, $b - y$, β , and HP2 are available for almost all stars, resulting in an average over four estimates (though the errors in T_{β} result in low weight for the β index), with additional data from V-R and R-I being available for roughly half of the sample.

6. The Observed and Intrinsic Spreads in Lithium Abundance

Figure 6(a) presents the lithium equivalent widths, \bar{W} , as a function of effective temperature. As the Li line is weak, its equivalent width varies linearly with abundance, so $\lg \bar{W}$ is linear in logarithmic abundance. In Fig. 6(b), the solid curve corresponds to the lithium abundance $A(\text{Li}) = 2.11$, based on the computation using Bell models at $\lg g = 4.0$ and $[\text{Fe}/\text{H}] = -2$ presented by Ryan et al. (1996a, Table 5). Individual abundances are shown in Fig. 6(c). The ultra-Li-weak star G186-26 is not shown in these figures.

The random error in each abundance measurement is taken to be the quadratic sum of the components due to errors in W and in the estimated temperature,

$$\sigma_{\text{err}}^2 = \left(\frac{\partial A}{\partial \lg W}\right)^2 \sigma_{\lg W}^2 + \left(\frac{\partial A}{\partial T}\right)^2 \sigma_T^2$$

Although we compute the error for each star individually, it is useful to make a general estimate of σ_{err} for the ensemble using mean values from Table 2: $\langle \bar{W} \rangle = 21 \text{ m}\text{\AA}$, $\langle \sigma_{\bar{W}} \rangle = 1.3 \text{ m}\text{\AA}$, and $\langle \sigma_T \rangle = 32 \text{ K}$. Since $\frac{\partial A}{\partial T} = 0.00065 \text{ dex K}^{-1}$ for turnoff stars, we expect $\sigma_{\text{err}} \simeq 0.033 \text{ dex}$.

The standard deviation of the 22 observations is $\sigma_{\text{obs}} = 0.053 \text{ dex}$. the dispersion found by Thorburn (1994), who viewed the dispersion as significant, and by Spite et al. (1996) and Bonifacio & Molaro (1997), who claimed the dispersion was within their errors. The study by Deliyannis et al. (1993) noted a range of possible dispersions depending on the composition of the sample.

The value $\sigma_{\text{obs}} = 0.053 \text{ dex}$ includes the contributions of quantifiable uncertainties in the data. We also need to consider the possibility that we have observed an admixture of stellar types not purely representative of Li plateau stars. On the second point, a striking feature of the observations is that the vast majority of the stars, 20 of the 22 measurements, fall within 0.1 dex of the mean. The form of the distribution is shown in Fig. 6(d), as

both a histogram and a stripe plot, the latter avoiding the undesirable effects of binning. These suggest a roughly Gaussian distribution about the mean with a small dispersion, plus two stars lower in abundance by $\simeq 0.14$ dex. Indeed, the standard deviation for the 20 stars within ± 0.1 dex of the mean is a mere $\sigma_{\text{obs}} = 0.036$ dex. The two stars with lower abundances therefore represent 4.1σ (CD–24°17504) and 3.4σ (BD+9°2190) deviations, address the reasons they differ below, but for now we emphasise that for 20 of the 23 stars in Table 2, i.e. for 87% of the very metal-poor, halo-turnoff sample, the observed spread in Li abundance is only $\sigma_{\text{obs}} = 0.036$ dex. Since we estimated the random error for the ensemble to be $\sigma_{\text{err}} = 0.033$ dex, it is clear that the vast majority of the sample is consistent with essentially zero scatter about the mean. In other words, *the Spite Li plateau is ultra-thin at the metal-poor turnoff*.

Three stars are highlighted in Fig. 6 and Fig. 7, where the latter shows the scatter about the Li plateau in standardised units $Z_i = (A(\text{Li})_i - 2.11)/\sigma_{A(\text{Li})_i}$. Two of the stars were introduced above. BD+9°2190 falls well below the mean, but by only 2.8 times its formal error, so its position could be consistent with its errors. In contrast, CD–24°17504 and CD–71°1234 lie away from the mean by (respectively) 4.7 and 3.5 times their formal errors, suggesting that they have genuinely different Li abundances from the rest. In §4.2.3, we searched for but failed to find evidence that the formal error estimates were unreasonable; it would be ad hoc, without more evidence, to suggest that these two stars are exceptions, especially since each has several observations. Even exclusion of CD–24°17504’s most extreme datum — 1997: $W = 15.1$ mÅ — would leave the star below the mean by 3.0 times its (revised) formal error. We conclude that both stars lie significantly away from the mean, and discuss the cause of this below (§7.3.1).

7. Discussion

7.1. Comparison with Previous Measurements of Spread

The essentially zero spread found for the Li plateau at the very metal-poor turnoff may be contrasted with larger values found in several previous studies.

Spite et al. (1996) and Bonifacio & Molaro (1997) both considered the spread they measured to be consistent with zero to within their formal errors. Our new result offers no contradiction, but due to the much better precision achieved in our study, $\sigma_{\text{err}} \simeq 0.033$ dex compared with 0.06–0.08 dex (Spite et al.) and 0.07 dex (Bonifacio & Molaro), our result can be stated much more strongly. Our better precision derives from the use of a very homogeneous data set, the checks undertaken to ensure that error estimates were appropriate (e.g. through double-blind processing and double measuring of every spectrum), the utilisation of multiple indices to minimise random errors in effective temperature, and the application of restrictive selection criteria which minimised physical differences between the stars. Otherwise, star to star differences might have induced greater temperature and/or metallicity dependent errors associated with color-effective temperature transformations and model atmospheres. We cannot claim that our abundance calculations have completely overcome the systematic errors — we quantify them in §7.7 — but we have avoided them insofar as they affect measurements of the thickness of the Li plateau.

Given the essentially zero intrinsic scatter found for our sample, how are we to interpret the earlier measurements of significant scatter by Deliyannis et al. (1993) and Thorburn (1994)? We reexamine these studies in reverse chronological order.

Thorburn (1994) acquired an almost homogeneous data set, making extensive observations (utilising four different telescope/spectrograph combinations) and quoting formal errors in the range 0.08–0.09 dex. Although the bulk scatter in abundances was 25%, this reduced to 15% once T_{eff} and [Fe/H] trends were removed. It is this latter figure which is relevant to the thickness of the Li plateau. Thorburn noted that the total formal

error would have to be increased by $\sim 20\%$ to explain the observed scatter, $\simeq 0.1$ dex, and suggested that the scatter may be a consequence of dispersion in the halo age-metallicity relationship and Galactic chemical evolution. However, the much smaller scatter we have found, $\simeq 0.03$ dex, obviates the need for such an explanation. We cannot be certain of the reason for the excess scatter in Thorburn’s study, but we argue as follows that it may be artificial. Four different instrumental setups were used, but neither sky nor scattered light subtractions were made, which Thorburn estimated could introduce errors of not more than 1–2% and possibly 3–5% respectively. It is conceivable that differences between the scattered light and sky backgrounds from telescope to telescope and from night to night have contributed to the scatter in the data. From Thorburn’s Table 2, the formal $\sigma(W)$ is typically only 10% of W . The errors from neglect of sky and scattered light will contribute 0% of W in the optimistic case and 7% of W in the pessimistic case, so the actual errors should be higher than the stated values by between 1.0 and 1.7 times. It is conceivable that the stated $\sigma(W)$ values do underestimate the actual errors in W sufficiently to explain the 1.2 times higher than expected scatter.

Deliyannis et al. (1993) studied an inhomogeneous compilation of data from the literature, and quantified the uncertainties of each measurement using a noise model of the type discussed above (e.g. Cayrel 1988). They considered a number of subsamples, and found a dispersion of $\pm \geq 20\%$ (2σ), i.e. $\sigma \geq 0.04$ dex, depending on which subsample was examined. This dispersion is not much different from our observed scatter, but as noted already, our formal errors are also at this level, so we infer < 0.02 dex intrinsic scatter. They computed the scatter in each sample at uniform $b - y$ color, which can be viewed as removing trends in T_{eff} but not trends in $[\text{Fe}/\text{H}]$. Claims of a dependence of $A(\text{Li})$ on $[\text{Fe}/\text{H}]$ had not been published at the time of the Deliyannis et al. work. With the benefit of hindsight, we might expect that the Deliyannis et al. scatter measurements could be inflated by the presence of such a trend, if it exists. (We will return to that point below.)

Subsequently, Thorburn (1994) estimated the [Fe/H] dependence of the $A(\text{Li})$ trend as 0.13 dex per dex; Ryan et al. (1996a) derived a similar value, 0.11. The Deliyannis et al. sample ranged from $-3.5 \leq [\text{Fe}/\text{H}] \leq -1.4$, which would span 0.25 dex in $A(\text{Li})$ if the slope noted above were correct. A normally distributed sample has a standard deviation $\sim 1/6$ to $1/4$ of its range, so a sample spanning 0.25 dex might well be expected to yield a standard deviation of 0.04–0.06 dex. Thus the scatter derived by Deliyannis et al. is consistent with published values of the embedded metallicity dependence of $A(\text{Li})$ and with the abundance range of their sample.

This explanation of Deliyannis et al.’s findings would fail, however, if the metallicity trend did not exist, as Bonifacio & Molaro (1997) concluded. We revisit this below (§7.3). Bonifacio & Molaro also pointed out that both Thorburn’s and Deliyannis et al.’s work used straight line fits to the data in determining the scatter, whereas exponential fitting functions may have been more appropriate. Although theoretically a non-linear form may have been better suited, it is not clear quantitatively whether the difference can be explained in this fashion.

7.2. Reexamination of G64-12, G64-37, and CD–33°1173

Ryan et al. (1996a) drew particular attention to G64-12, G64-37, and CD–33°1173 as three stars having essentially identical atmospheric parameters but irreconcilable lithium abundance determinations. All three stars are included in the present study, and as the conclusions already stated indicate, we no longer identify a significant spread amongst this set of stars. The effective temperatures (Table 2) are still within a total range of 30 K, and the metallicities (Table 1) are within 0.10 dex. However, the homogeneous Li equivalent widths we have measured in this work differ considerably from those in the heterogeneous compilation of Ryan et al. The new vs old values (in mÅ) are respectively:

G64-12, 21.1 ± 1.1 vs 27 ± 1.8 ; G64-37, 18.2 ± 1.5 vs 15 ± 1.0 ; and CD-33°1173, 17.2 ± 1.2 vs 12 ± 1.2 . The formal errors in the current work differ little from the 1996 compilation, but in view of the homogeneity which we have achieved in the new data set, we prefer the newer measurements. We have no detailed explanation for the discrepancy other than to repeat the cautions given in Ryan et al. (1996a) and elsewhere that it is easy to overlook or misjudge error contributions when making error estimates and combining heterogeneous data sets.

7.3. Examination of $A(\text{Li})$ vs [Fe/H]

7.3.1. Morphology of the Sample

Trends of $A(\text{Li})$ with both T_{eff} and [Fe/H] were cited by Norris et al. (1994), Thorburn (1994), and Ryan et al. (1996a). However, Bonifacio & Molaro (1997) concluded that these were eliminated by using the IRFM temperatures of Alonso, Arribas, & Martinez-Roger (1996b).

We chose our sample to be very metal-poor, both to minimise the differences between stars in the study and to obtain measurements of objects which show the least signs of chemical enrichment. However, the stars do span a small range of metallicity and, given the proven accuracy of the data, are useful for examining again the metallicity dependence of $A(\text{Li})$. We plot Li abundance vs [Fe/H] in Fig. 8(a). Recall from §3 that the [Fe/H] values are mostly based on high and/or medium-resolution spectroscopic observations, for which $\sigma_{[\text{Fe}/\text{H}]} \simeq 0.15$ dex. It is clear at first glance that a similar trend with [Fe/H] is identified in the present study as was measured by Thorburn (1994) — 0.13 dex per dex — and by Ryan et al. (1996a) — $0.111 \pm 0.018(1\sigma)$. An ordinary least squares (OLS) fit, excluding only G186-26, gives $dA(\text{Li})/d[\text{Fe}/\text{H}] = 0.121(\pm 0.028)$ (errors are standard errors), with a

scatter about the trend $\sigma_{\text{obs}} = 0.037$ dex (dotted line, Fig. 8(a)). Moreover, although we discussed above whether CD–24°17504 and CD–71°1234 should be included or excluded, it is clear that they lie on the *same* trend as the rest of the data in Fig. 8(a). This justifies our confidence in the quality of the observational data.

Because of possible concern whether the trend is real or illusory, we undertook a series of regression analyses, excluding a priori G186-26. These included ordinary least squares (OLS), reweighted least squares (RWLS — Rousseeuw & Leroy 1987), which is a robust technique that detects outliers, the BCES⁵ approach adopted by Bonifacio & Molaro (1997), which has regard for the various error contributions in each datum, and a robust technique based on a bisquare regression procedure described by Li (1985). The first step was to undertake OLS and RWLS bivariate analyses of $A(\text{Li}) = a_0 + a_1 \times [\text{Fe}/\text{H}] + a_2 \times T_{\text{eff}}$. Detailed results are presented in Table 5. The coefficient of determination, R^2 , listed in the table indicates the proportion of variance in the dependent variable which is explained by the independent variable(s) in the regression model. For both techniques, and also for culled subsets of the data, we found the coefficient of T_{eff} to be indistinguishable from zero, to a precision of $\simeq 0.010$ (1σ) dex per 100 K. This is not *entirely* surprising given the short temperature interval for the data, but is nevertheless inconsistent ($>3\sigma$) with the result of a previous analysis of heterogeneous data (Ryan et al. 1996). The bivariate RWLS analysis rejected BD+09°2190 as an outlier, but this did not alter the redundant status of the T_{eff} coefficient. Whatever the explanation for the difference between the Ryan et al. (1996) sample and the current one, clearly a temperature term is unnecessary in the present analysis, and all further tests were conducted using univariate fits of the form $A(\text{Li}) = a_0 + a_1[\text{Fe}/\text{H}]$.

The OLS univariate fit to the data is shown as a dotted line in Fig 8(a). The RWLS fit

⁵Bivariate Correlated Errors and intrinsic Scatter (Akritas & Bershady 1996)

again identified BD+9°2190 as an outlier, and the fit to the remaining stars is shown with the solid line. This represents our “best fit” —

$$A(\text{Li}) = 2.447(\pm 0.066) + 0.118(\pm 0.023) \times [\text{Fe}/\text{H}].$$

(The RWLS regression is identical to that which would be obtained from the OLS fit if BD+9°2190 was excluded a priori.) Clearly, the result is barely sensitive to the inclusion or exclusion of this star. The coefficient of [Fe/H] is found to be non-zero at a high significance, viz. $0.118 \pm 0.023(1\sigma)$. The same conclusion was reached from the assortment of other regression tests preformed (see Table 5 for details).

Earlier in the discussion, we identified CD−24°17504 and CD−71°1234 as deviating from the mean by more than their formal errors. This can now be understood in terms of their rankings at the low and high end of the metallicity scale. Although they were not identified as outliers by the RWLS fit, we considered further the possibility that they might carry excessive weight in influencing the trend, and conducted tests on a culled sample. A RWLS regression from which BD+9°2190 was culled a priori subsequently identified CD−24°17504 and CD−71°1234 as outliers, and gave a shallower, but still significantly non-zero, slope for the trend —

$$A(\text{Li}) = 2.318(\pm 0.063) + 0.073(\pm 0.022) \times [\text{Fe}/\text{H}].$$

The fit for the culled sample is shown in Fig. 8(e). Alternative regression fits for this sample are given in Table 5; all give significantly non-zero values for the slope.⁶

⁶We note for completeness that the star HD 74000, which fell outside the metallicity and temperature range of our sample selection criteria, was nevertheless observed as a standard star, in order that we could compare our equivalent width measurements with those of other workers. We noticed, however, that it has a lower $A(\text{Li})$ abundance than most other stars in

Figure 8(b) and 8(f) give the residuals of $A(\text{Li})$ about the regression functions, with open circles indicating data excluded from the fit. Histograms and stripe plots (Fig. 8(c) and 8(g)) show the residual distributions. The “best fit” yields a dispersion

$$\sigma_{\text{obs}} = 0.031 \text{ dex},$$

while the “culled fit” has $\sigma_{\text{obs}} = 0.024$ dex. Robust biweight estimators of scale (see Beers, Flynn & Gebhardt (1990) and references therein) yield values $S_{BI} = 0.031$ and 0.025 respectively. (The biweight estimate of scale converges to the standard deviation estimator when sampling from a normal distribution, but is less sensitive to the presence of outliers). The normality of the $A(\text{Li})$ residuals is established not only by the excellent agreement between the σ and S_{BI} values, but also via the lack of departure from linearity in the “normal probability plots⁷” in Fig. 8(d) and 8(h).

The regression analysis may be summarised thus: We have found a positive dependence of $A(\text{Li})$ upon $[\text{Fe}/\text{H}]$ (but not T_{eff}) which resembles the values found previously by Thorburn

our sample. If it had been included in the target group, it too would have been rejected by the outlier-detection routines in our regression analyses. If ${}^7\text{Li}$ is genuinely depleted in this star, this may account for the non-detection of ${}^6\text{Li}$ despite it being only 100 K cooler than HD 84937 and BD+26°3578 in which ${}^6\text{Li}$ is seen (Smith et al. 1998).

⁷A normal probability plot ranks the data from lowest to highest, and plots the ordered value against its theoretical Z-statistic. The Z-statistic gives the number of standard deviations by which the datum would depart from the mean in a normal distribution of N points. For a normal distribution, ranked datum i will possess probability value $i/(N+1)$ measured from the lowest tail, so the cumulative probability distribution is inverted to find the corresponding Z-statistic. If a data set is normally distributed, then it will lie about a straight line in the plot, whereas an asymmetric distribution will deviate from the line along a curved path. See, e.g., Levine, Berenson & Stephan (1998).

(1994) and Ryan et al. (1996). Our best fit gives $dA(\text{Li})/d[\text{Fe}/\text{H}] = 0.118(\pm 0.023)$. Shallower values of the slope can be obtained by a priori rejection of some of the data — which may be an invalid action — leading to $dA(\text{Li})/d[\text{Fe}/\text{H}] = 0.073(\pm 0.022)$, but even then the slope is significant at $\geq 3\sigma$. The scatter measured for the best fit is $\sigma_{\text{obs}} = 0.031$ dex. Obviously, rejection of stars to obtain a shallower slope yields even smaller values of the scatter, but in any case the observed scatter is consistent with the expected errors $\sigma_{\text{err}} \simeq 0.033$.

7.3.2. *Is the Trend Natural or Artificial?*

A major similarity between the Ryan et al. (1996a) study and the present one is the use of the same computations relating equivalent width to abundance. If a metallicity-dependent error existed in that work, it would persist here. Can such an error be identified?

The Ryan et al. (1996a) work used model atmospheres from Bell (1983), computed at $[\text{Fe}/\text{H}] = -2$. If the model structure differed sufficiently for real stars between $[\text{Fe}/\text{H}] = -3.0$ and -2.0 , a metallicity dependent error might be expected. However, the Kurucz (1993) models (which extend to lower abundance than Bell's but have high convective overshoot) show that changing from the higher to the lower metallicity would change the inferred Li abundance by only 0.012 dex (see Ryan et al. 1996a, Fig. 2). This is an order of magnitude less than the trend identified and a factor of three smaller than σ_{obs} , and in the sense of steepening rather than flattening the trend. On this estimate, the atmospheric models are not sufficiently sensitive to metallicity to produce the trend we observe. Note also that Thorburn used Kurucz (1993) models rather than the Bell models as adopted here, yet derived an almost identical trend. This emphasises again that selection of a different model grid may alter the derived absolute abundance, but will have little effect on the differential characteristics of the results.

An alternative source of error might be a metallicity dependence in the effective temperature scale. Our effective temperatures were based substantially on B–V, $b - y$, and HP2. In §5 we argued that all of the indices used are insensitive to metallicity for very low-metallicity turnoff stars. An error of 100 K in effective temperature would produce an abundance error of 0.065 dex for stars of the temperature and metallicity of our sample, so an error of 200 K would have to be induced *over the short metallicity interval from $[Fe/H] = -2.3$ to -3.5* to produce the trend observed, yet we identified at worst an 18 K change in the Kurucz (1993) color transformations. In view of the lack of sensitivity of our temperature indicators for the types of stars investigated, we do not believe that the trend can be explained away in this fashion.

We have ruled out metallicity-dependent errors in the stellar atmospheres and effective temperature scales as causes of the trend. We do not expect such errors in the equivalent width measurements either, since the spectra are devoid of lines around Li 6707 Å and the continuum fit should be reliable irrespective of metallicity for our stars. NLTE effects were assessed and rejected as the cause by Ryan et al. (1996a). We are left with little alternative but to restate our identification of the trend over the interval $-3.6 < [Fe/H] < -2.3$, and to consider it to be natural until proved otherwise.

7.3.3. The Bonifacio & Molaro Analysis in Retrospect

The metallicity dependence derived here is very similar to that found by Ryan et al. (1996a) and Thorburn (1994), but the new sample is far more homogeneous and of much higher quality. How then should we view Bonifacio & Molaro’s (1997) conclusion that there is no metallicity dependence? Their work used IRFM temperatures, which one might arguably prefer over other scales, especially as far as systematic errors are concerned, but there are two crucial disadvantages of their study compared with ours. Firstly, the formal

errors in the IRFM temperatures listed by Bonifacio & Molaro are typically 80 K, whereas by averaging many different indices we have reduced the random error to typically 30 K. The larger errors of the IRFM temperatures induce greater random scatter about the Li plateau for that dataset. Secondly, their equivalent widths and [Fe/H] values were based on a literature survey of inhomogeneous and less reliable data than in our new work. The combined effect of these factors is that, although their bivariate fit of $A(\text{Li})$ on [Fe/H] and T_{eff} gave a slope consistent with zero, the uncertainty in its determination was sufficiently large that our new value lies at only their 2.5σ tolerance⁸. Bonifacio & Molaro’s univariate fits, however, are irreconcilable with our result, having [Fe/H] coefficients ranging from -0.02 to -0.05 dex per dex and uncertainties (1σ) of 0.03 to 0.06 dex per dex, depending on the statistical test. In what follows, we identify additional reasons for the differences between their result and ours obtained with the current sample.

The difference between our estimated slope of $A(\text{Li})$ on [Fe/H] and that of Bonifacio & Molaro can be explained upon closer scrutiny of the literature data used in their study. Figure 9 shows the subset of nine stars common to both works. We use the new homogeneous $W(\text{Li})$ values from this study, but show abundances calculated on both the IRFM and our temperature scales (central and upper panels respectively). We plot these against both the literature [Fe/H] values referenced in Table 2 (left hand panels) and the values used by Bonifacio & Molaro (right hand panels). The effect of using the IRFM scale is to generate huge scatter (central panels) due to the low precision of those individual values. As emphasised previously, high internal precision is required to assess the spread about the Li plateau, and this precision is delivered by the variance⁻¹-weighted average over three to six different temperature indicators, not by the use of a single “noisy” index

⁸Their bivariate fit for an LTE analysis without depletion corrections (i.e. matching our assumptions) gave a metallicity slope 0.034 ± 0.034 dex per dex.

even if the latter may have better systematics.

Restricting our attention, then, to the low scatter (uppermost) panels using the temperatures computed in this work, it is clear that the trend with metallicity depends on the adopted metallicity estimates. Without more information, it would not be possible to know whether the literature [Fe/H] compilation in Table 2 or that used by Bonifacio & Molaro is better. Fortunately, we do have more information, in the second set of [Fe/H] values derived from applying the calibration of Beers et al. (1999) to our 1Å-resolution spectra (see Table 2). In the bottom panels of Fig. 9, we compare the metallicities derived from those 1Å-resolution spectra with the adopted literature values (Fig. 9(e)) and those used by Bonifacio & Molaro (Fig. 9(f)), and find excellent agreement with our adopted literature values, but considerable disagreement with some of the values adopted by Bonifacio & Molaro, to the extent that the plot in Fig. 9(b) becomes levelled off by the scatter in [Fe/H]. For completeness, we note that an OLS regression of our presently derived $A(\text{Li})$ estimates with the Molaro & Bonifacio values of [Fe/H] for the nine stars in common (Fig. 9(b)) results in a slope with respect to abundance of 0.008 (+/- 0.041), i.e., completely consistent with zero. However, on the basis of these comparisons, we favor the literature [Fe/H] values adopted in Table 2 to those adopted by Bonifacio & Molaro. Preferring also the temperatures derived from multiple indices rather than the individual temperatures based on the IRFM, we believe that Fig. 9(a) is the most reliable presentation of the data.

Restating our result above, allowing for the [Fe/H] dependence in our sample with only G186-26 and BD+9°2190 excluded, *we find a tiny dispersion, $\sigma_{\text{obs}} = 0.031 \text{ dex}$, for 91% of the sample*. It remains now to discuss the significance of the trend with metallicity.

7.4. ${}^6\text{Li}$ as a Tracer of Non-Primordial ${}^7\text{Li}$

The interpretation of halo Li abundances would be greatly simplified if the Spite Li plateau had no dependence upon metallicity. However, we have again measured a positive dependence. Furthermore, and even if one denies the reality of this trend, the fact that at least two stars in our sample are contaminated with ${}^6\text{Li}$ indicates a distinctly non-primordial origin for *some* of the Li in these stars. Smith, Lambert, & Nissen (1993, 1998) and Hobbs & Thorburn (1994, 1997) have measured the presence of ${}^6\text{Li}$ in HD 84937 and BD+26°3578 at the level of ${}^6\text{Li}/\text{Li} = 0.06 \pm 0.03$ and 0.05 ± 0.03 (Smith et al. 1998) respectively. Both of these stars are in our sample. Our data are not of high enough resolving power or S/N to measure ${}^6\text{Li}$ separately, but since all of the stars in our narrowly-defined sample should have a similar evolutionary history and stellar structure, more likely than not they will all be contaminated by ${}^6\text{Li}$.

In the following discussion, we assume that all of the ${}^6\text{Li}$ is pre-stellar. Alternative possibilities were examined by Lambert (1995), who performed an initial appraisal of synthesis by Galactic cosmic rays stopped in the stellar convection zone, and by Deliyannis & Malaney (1995), who considered synthesis by stellar flares. The former appraisal revealed potentially important production of ${}^6\text{Li}$, but with large uncertainties, and on balance Lambert viewed the mechanism as probably too inefficient. The second assessment indicated possibly significant levels of ${}^6\text{Li}$ production and retention in turnoff stars, but again the calculation was subject to large uncertainties associated with the (unknown) flare-history of the star.

As ${}^6\text{Li}$ production at the levels measured exceeds that expected from standard Big Bang nucleosynthesis, we infer that it originates in sources associated with Galactic chemical evolution (GCE), and we should expect GCE production to vary with [Fe/H]. Furthermore, since GCE ${}^7\text{Li}$ production must accompany GCE ${}^6\text{Li}$ production, we have to disentangle

three components to the abundances we measure via a single spectral feature: primordial ^7Li , GCE ^7Li , and GCE ^6Li .

Ramaty, Kozlovsky, & Lingenfelter (1996) and Ramaty et al. (1997) give the production ratio of $^7\text{Li}/^6\text{Li}$ as $\sim 1.3\text{--}1.7$ for Galactic cosmic rays having energies and compositions consistent with Be and B synthesis. We adopt the value 1.5 in the calculations that follow. Assuming $^6\text{Li}/\text{Li} = 0.05$, (i.e. $^6\text{Li}/(^6+^7\text{Li})$) and making the most conservative assumption that none of the pre-stellar ^6Li has been destroyed in these turnoff stars, we would argue that 8% of the ^7Li , and 13% of the total Li absorption in these stars is non-primordial. We would therefore infer that the primordial value of ^7Li should be 0.06 dex lower than the observed $A(\text{Li})$. If some of the ^6Li has been destroyed during these stars' lifetimes, as seems likely, then the GCE ^7Li fraction would be higher and the primordial value lower. Destruction of ^6Li at the turnoff is predicted to be a strong function of mass (effective temperature) and age, and standard Yale models (e.g. Deliyannis et al. 1990; Pinsonneault et al. 1992) show that depletion by 0.1 to 0.5 dex is not unreasonable, and that substantially more depletion may have taken place in practice. If we assume that 50% of the pre-stellar ^6Li has been destroyed, then the GCE ^7Li component would be 17% of the total; 21% of the current line absorption would be due to GCE, and the primordial value would be 0.10 dex lower.

7.5. Non-Primordial Li and the [Fe/H] Dependence

Since the presence of ^6Li indicates that at least some non-primordial Li is present, it is logical to ask whether the inferred GCE ^6Li and ^7Li components can explain the observed dependence of $A(\text{Li})$ on [Fe/H]. The calculations above show that the primordial ^7Li abundance probably is *at least* 0.06 dex lower than the $A(\text{Li})$ abundance measured in HD 84937 and BD+26°3568, and that a value 0.10 dex lower might be a realistic estimate. According to the measured trend, the [Fe/H] value at which $A(\text{Li})$ is observed to be 0.10 dex

lower than in the relatively metal-rich stars HD 84937 and BD+26°3568, is $[\text{Fe}/\text{H}] = -3.2$. It is important to note that we have argued elsewhere (e.g. Ryan et al. 1991, 1996b; Ryan 1996), in work *not* involving Li, that the Galaxy’s first supernova enrichment events give rise to stars around $[\text{Fe}/\text{H}] \sim -4.0$ to -3.5 . The metallicity dependence we have measured for Li is therefore roughly consistent with the GCE contribution to Li inferred up to the time when HD 84937 and BD+26°3568 formed. It is not unreasonable to suppose, then, that the most metal-poor star in our sample, CD-24°17504 with $[\text{Fe}/\text{H}] = -3.55$, has minimal GCE contribution to its Li line, whereas at higher metallicities we see the GCE contribution increasing.

If ${}^6\text{Li}$ preservation is confined to turnoff stars, as the Yale models suggest (Deliyannis et al. 1990; Pinsonneault et al. 1992), then in cooler dwarfs we would have to adjust only for GCE ${}^7\text{Li}$ to obtain the uncontaminated primordial value. However, since GCE ${}^6\text{Li}$ contributes less than GCE ${}^7\text{Li}$ to the contamination, the offset would be reduced only from 0.10 dex to 0.08 dex. This is not a major difference, but does emphasise that the metallicity dependence may be slightly weaker in dwarfs away from the turnoff.

We have argued that the observed metallicity dependence in this very metal-poor sample is consistent with the GCE contribution inferred from the ${}^6\text{Li}$ measurements in two stars at $[\text{Fe}/\text{H}] \sim -2.4$. However, if we are to claim to understand the slope as due to GCE and hence be able to infer that the most metal-poor stars yield the correct primordial Li abundance, then we also need to assess whether the explanation correctly predicts the metallicity dependence in more metal-rich stars. Smith et al. (1998), amongst others, have noted that if the Li/Be ratio is maintained in GCE production throughout formation of the halo, then the Galaxy ought to have become very rich in Li by $[\text{Fe}/\text{H}] = -1$, but apparently it did not. The $\alpha + \alpha$ fusion mechanism produces roughly uniform Li throughout the phase of halo formation in contrast to the strong metallicity dependence of Be and B (Steigman

& Walker 1992), and Olive & Schramm (1992, eq. (6)) predict, by comparing Li to Be, a very shallow relationship, approximately GCE $A(^7\text{Li}) \simeq 1.59 + 2Z/Z_\odot$ for $Z/Z_\odot < 0.1$. Clearly, however, the detailed evolution of ^6Li , and therefore of GCE ^7Li , also depends on the chemical evolution model adopted (e.g. Prantzos, Casse, & Vangioni-Flam 1993; also contrast Figs 1 and 2 of Yoshii, Kajino, & Ryan 1997). The lesson from these models is that the inferred total Li abundance need *not* climb significantly more steeply over the range $-2.5 < [\text{Fe}/\text{H}] < -1.5$ than it does over the interval $-3.5 < [\text{Fe}/\text{H}] < -2.5$ which we have measured. Furthermore, since the higher-metallicity samples often include cooler stars, the average observed slope may flatten slightly at higher metallicity due to the erasure of the ^6Li contribution to $A(\text{Li})$.

In summary, we regard the slope in $A(\text{Li})$ vs $[\text{Fe}/\text{H}]$ to be concordant with the amount of GCE inferred from the observed ^6Li abundances. Furthermore, GCE models which have higher Li/Be yields at lower metallicity (e.g. Steigman & Walker 1992) suggest that the amount of GCE Li expected at higher metallicities need not invalidate this explanation. Irrespective of whether the metallicity trend is believed (since there may be sceptics in the readership), from the observed ^6Li fractions we infer that the primordial abundance is $\simeq 0.10$ dex below that with which stars having $[\text{Fe}/\text{H}] \sim -2.4$ were born.

In addition to the galactic cosmic ray mechanism discussed above, stellar nucleosynthesis of ^7Li may contribute to the measured trend. D'Antona & Matteucci (1991) computed an increase of $A(\text{Li})$ by 0.17 dex over the interval $[\text{Fe}/\text{H}] = -2.5$ to -1.5 , for production in $2-8 M_\odot$ AGB stars. Although that slope is subject to uncertainties in the adopted parameters — they also computed models which showed steeper trends — and could be less, it emphasises that even at this early stage of GCE, we must recall the *likelihood*, not merely the *possibility*, that the Li we observe in halo stars is affected by GCE. The trend we have measured, 0.12 dex per dex, is concordant with the observed ^6Li contamination

and expected stellar production.

Before leaving this discussion, we note that the narrowness of the Li spread is maintained over the range $[\text{Fe}/\text{H}] < -2.3$, even though GCE is leaving its mark on material, increasing $A(\text{Li})$ and producing measurable ${}^6\text{Li}$. This result sets an additional constraint on GCE models of lithium processing. One interpretation is that any age spread in the formation of halo stars over this low-metallicity interval must not be so great as to lead to expectations of a measurable range of $A(\text{Li})$ at a given $[\text{Fe}/\text{H}]$. However, an inference on age ranges may be relaxed in the Searle & Zinn (1978) framework where early halo star formation began in separate, independently evolving fragments. In these first star formation events in the voluminous proto-halo, it is possible that regions were sufficiently separated that cosmic rays accelerated in one part did not reach and induce reactions in the others, so Li would evolve in concert with the local metallicity rather than the galactic age. Unfortunately, models of cosmic ray propagation in the voluminous proto-halo are less well constrained than in the Galactic disk, for which we can infer present day lifetimes, path lengths and spectra. The measurement of ${}^6\text{Li}$ in more halo stars will help constrain the Galactic cosmic ray production ratios ${}^{6,7}\text{Li}/\text{Be}$ and ${}^{6,7}\text{Li}/\text{B}$ in the earliest phase of GCE.

7.6. Constraints on Rotationally Induced Mixing Models

The rotationally-induced turbulent mixing models of Pinsonneault et al. (1992) differ from the Yale “standard” and “diffusive” models in predicting substantial (~ 1 dex) depletion of Li in halo turnoff stars. Amongst the signatures of this depletion mechanism are a mildly-arched “plateau” and a spread in final abundances reflecting the range of initial angular momenta of the stars.

Using updated models having an improved treatment of the evolution of angular

momentum, and considering the spread in $A(\text{Li})$ seen in Thorburn’s (1994) data, Pinsonneault et al. (1998) concluded that the mean Spite Li plateau abundance was depleted by 0.2–0.4 dex from the primordial value. Utilising our more accurate data for turnoff stars, we now revisit that result.

Pinsonneault et al. (1998) computed the depletion $-\log D_7 = A(\text{Li})_{\text{final}} - A(\text{Li})_{\text{initial}}$ for stars with $[\text{Fe}/\text{H}] = -2.3$ and $T_{\text{eff}} = 6000$ K, coincidentally very similar to the parameters typical of our sample. They present their results for three different solar angular momentum histories (which affect the calibration of their models), convolved with observational errors of 0.00 and 0.09 dex corresponding to perfect observations and the formal error of Thorburn (1994) respectively. As our formal errors are only 0.033 dex, we broadened Pinsonneault et al.’s “perfect”, minimal depletion “s0” model by an appropriate value, and compare it to our data in Fig. 10(a). (Recall that G186-26 is heavily depleted and lies offscale.) The depletion curves and data are brought into coincidence by assuming an initial abundance $A(\text{Li})_i = 2.22$ dex. It appears at first sight that the data are clustered more tightly than the theoretical boundaries enclosing $\pm 47.5\%$ of the population (dashed curves). However, it is more reliable to view the distributions functions directly, so we have renormalized the theoretical distribution with zero observational error (Pinsonneault et al., Fig. 9(a)) to the number of stars in our sample, and scaled the depletion from their $T_{\text{eff}} = 6000$ K to the mean of our sample, $T_{\text{eff}} = 6200$ K. Our raw sample (excluding only G186-26), shown in Fig. 10(b), not surprisingly has a broader core than the theoretical distribution because of the imbedded $[\text{Fe}/\text{H}]$ trend. Fig. 10(c) overcomes the trend by shifting all stars to a common metallicity — $[\text{Fe}/\text{H}] = -2.8$, the median value of our sample — using $\Delta A(\text{Li})/\Delta [\text{Fe}/\text{H}] = 0.12$. The cores of the observed and theoretical distributions match well, but the model has a Li-depleted tail extending to much lower abundances than the data. Specifically, Fig. 10(c) showing Pinsonneault et al.’s (1998) model “s0” with least depletion, predicts that 17% of the sample, or 3.9 stars for our sample of 23, will have

$A(\text{Li}) < 2.0$ (at $[\text{Fe}/\text{H}] = -2.8$). In fact we observe only one star below this limit, G186-26, and even that is excessively depleted compared to the model, as if some factor other than the Pinsonneault et al. mechanism is responsible. We conclude that even the minimally depleting “s0” model of Pinsonneault et al. overpredicts the degree of Li depletion in the turnoff stars. Whereas the Thorburn sample allowed Pinsonneault et al. to infer depletion by 0.2–0.4 dex by this mechanism, the higher quality data now available give rise to two new conclusions: (1) even the “s0” rotational model with a median depletion as small as 0.1 dex at $T_{\text{eff}} = 6200$ K predicts a broader spread than permitted by the turnoff observations; and (2) the very low Li abundance in G186-26 is not consistent with the rotational-depletion distribution function. The latter result signals that this star, and consequently the other ultra-Li-depleted halo dwarfs, do not represent the tail of a rotational depletion distribution. It is no longer possible to infer a minimal rotational depletion of 0.2 dex as Pinsonneault et al. were led to do with less accurate data.

The extremely tight clustering of the halo turnoff stars therefore presents a serious challenge to inferences from *this* class of models that the turnoff stars have depleted by even as little as 0.1 dex from a higher initial value.

7.7. The Primordial ^7Li Abundance

Several estimates of the primordial Lithium abundance, $A(\text{Li})_p$, can be made from the discussion above. They are: (A) $A(\text{Li})_p$ is $\simeq 0.10$ dex below that observed in HD 84937 and BD+26°3578, using the ^6Li observations and depletion estimates to infer the underlying primordial ^7Li value; (B) it is the value measured in the most metal-poor star of the sample, CD-24°17504 at $[\text{Fe}/\text{H}] = -3.55$, whose metals reveal a minimally-processed sample of early Galactic material; or (C) it is the extrapolation of the metallicity trend to $[\text{Fe}/\text{H}] = -4$ where the most metal-poor stars known are found and where the metallicity distribution of

the halo shows signs of truncation (Beers et al. 1998; Norris 1999). The values obtained are $A(\text{Li})_p = 2.06$ (A), 1.97 (B), and 1.98 (C). That is, *we infer that the primordial abundance is $A(\text{Li})_p \simeq 2.00$, and that future measurements of stars with $[\text{Fe}/\text{H}] < -3.0$ will yield values of $A(\text{Li})$ lower than the bulk of the present sample* (for which $A(\text{Li}) \simeq 2.1$), concordant with the trend shown in Fig. 8(a). What uncertainties should we attach to our estimate of the primordial value? We refer readers to the comprehensive discussion of errors by Thorburn (1994, §5) and to our previous works (Norris et al. 1994; Ryan et al. 1996a), and summarise below the results most relevant to the present discussion.

We have previously noted that typical random errors in our estimation of $A(\text{Li})$ are $\sigma_{\text{err}} = 0.033$ dex. Amongst systematic errors, Thorburn gives the uncertainties in oscillator strengths as $\sigma \simeq 0.02$ dex. A 0.5 dex error in $\lg g$ would produce < 0.01 dex error in $A(\text{Li})$ at the turnoff. Reasonable uncertainties in microturbulence and the damping coefficient are similarly unimportant due to the dominance of thermal broadening in the core of this weak line of a species with such low atomic mass. Corrections for NLTE are -0.01 at 6100 K and -0.03 dex at 6300 K (for $[\text{Fe}/\text{H}] = -2$ and $\lg g = 4$; Carlson et al. 1994). Far greater systematic uncertainties arise due to the uncertainties in the zeropoint of the effective temperature scale and the model structures. In §5.3, we found it necessary to make zeropoint adjustments to the various scales by as much as 165 K, which for the turnoff stars corresponds to an $A(\text{Li})$ change of 0.11 dex. A similar difference arises in the abundances derived from the Bell models compared with those from Kurucz's (1993) convective overshoot models, the latter giving $A(\text{Li})$ higher by 0.08 dex at the turnoff (Ryan et al. 1996a, §3.3). Bonifacio & Molaro's (1998) study of the Li 6140 Å line in HD 140283 shows that abundances derived from the 6707 Å resonance doublet are not grossly in error.

Since $\sigma_{\text{obs}} = 0.031$ dex and $\sigma_{\text{err}} = 0.033$ dex, we have established that there is no intrinsic spread about the Li plateau at the metal-poor turnoff, to a level $\sigma_{\text{int}} < 0.02$ dex. It

is clear that the absolute uncertainties in the primordial abundance are dominated not by random errors but by four systematic factors: (1) the zeropoint in the metal-poor effective temperature scales, $\simeq 0.1$ dex; (2) uncertainties in the metal-poor model atmosphere structures, $\simeq 0.1$ dex; (3) correction of the observed level for the contamination of GCE ^6Li and GCE ^7Li ; and (4) correction for any destruction of pre-stellar Li. Our three approaches (above) to account for the GCE fraction gave results ranging over 0.09 dex. That is, sources (1), (2), and (3) each contributes $\simeq 0.1$ dex to the systematic uncertainty in $A(\text{Li})_p \simeq 2.00$.

Until recently, source (4) was perhaps the most uncertain, since the degree of depletion predicted by models depends very much on the input physics. The simplest models predict essentially no destruction of Li (< 0.05 dex) at the metal-poor turnoff (Deliyannis et al. 1990), whereas rotationally-induced mixing led Pinsonneault et al. (1998) to infer destruction by 0.2–0.4 dex. However, the observations presented in this work set much tighter constraints on the degree of rotationally-induced mixing than the data available to Pinsonneault et al. could do, and on the basis of the very narrow scatter we have measured, we conclude that depletion by the rotationally-induced mixing mechanism is < 0.1 dex. Although this limit is more severe than Pinsonneault et al. were able to establish, it is consistent with Fields & Olive’s (1998) limit of < 0.2 dex depletion of ^7Li , argued on the basis of light isotope ratios.

Observations show that diffusion has not affected $A(\text{Li})$ (Ryan et al. 1996a), but it is unclear how diffusion is inhibited. Vauclair & Charbonnel (1995) suggest that *small* stellar winds balance diffusive effects while avoiding nuclear burning. Although the simplest models present an incomplete picture and fail to explain many behaviors (e.g. Deliyannis 1995), they may yet be giving the correct result for the turnoff stars. Certainly the thinness of the Li plateau argues against the models with rotationally-induced mixing, for which a larger spread in $A(\text{Li})$ is predicted. Economy of hypothesis in this situation suggests that

systematic error source (4) is rather small. However, Vauclair (1999) challenges empirical inferences of this sort in the face of current models in which depletion seems unavoidable. Another possibility requiring further study is discussed in §7.8.

We finish this section by noting that the essentially zero scatter found for the very metal-poor turnoff stars points strongly towards there having been a primordial value for ${}^7\text{Li}$, and near-elimination of the concerns over its depletion in these stars (but see Vauclair 1999 for an opposite view) suggests that we are now closer to identifying that value with confidence. Burbidge & Hoyle (1998) have considered that of the three factors: (a) stellar processing, (b) Galactic production, and (c) Big Bang nucleosynthesis, (c) is the one that has not operated. The results of the current study drive us to the contrary conclusion that (a) has not operated significantly, (b) can be constrained jointly by the ${}^6\text{Li}$ abundance of these objects and the measured dependence of $A(\text{Li})$ on $[\text{Fe}/\text{H}]$, and that (c) is the most likely cause for the near-uniformity first reported by Spite & Spite (1982), supporting their conclusion that the observed abundance was “hardly altered” from the primordial one.

7.8. The Spread in Lithium Abundances in Globular Clusters

A discussion of the spread of Li in field stars would not be complete without reference to the observations of Li in subgiants in the globular cluster M92 which show a range of $A(\text{Li})$ (Deliyannis et al. 1995; Boesgaard et al. 1998). Those authors considered whether various Li production mechanisms — the neutrino process in SN II, Galactic cosmic ray $\alpha + \alpha$ nucleosynthesis, and ${}^7\text{Be}$ transport in AGB stars — could account for the diversity, but in each case found requirements that violated other observational constraints, such as expectations of enhanced $[\text{Mg}/\text{Fe}]$ ratios, age spreads within the cluster itself, and enhanced abundances of s-process elements. They were driven to prefer scenarios in which the range of $A(\text{Li})$ reflected differential depletion from a higher abundance, rather than differential

enhancement from a lower level.

It is perhaps surprising that M92 reveals a spread in abundance of a factor of 2–3 for a small sample of stars, whereas in the field we find no spread ($\sigma_{\text{int}} < 0.02$ dex) for 91% of our sample. The mean metallicities of our samples are not greatly dissimilar, and the stellar masses must be almost identical since our sample is right at the turnoff and the M92 sample is on the subgiant branch. Moreover, the globular cluster sample should have an even narrower age distribution than the field sample. Either some feature of the globular cluster environment or the different post-main-sequence evolution of the subgiants must be responsible for the differences, assuming both data sets are reliable.

Can we reconcile Boesgaard et al.’s preference for a rotationally-induced depletion mechanism in the globular clusters with the absence of a spread in the halo? Possibly. If environmental factors are responsible for the difference, we may question whether the globular cluster members experience a very different history of angular momentum evolution, giving rise to a larger spread in $A(\text{Li})$. Certainly the suggestion of different angular momentum distributions between cluster and field star samples is not new. Peterson, Tarbell, & Carney (1983) and Peterson (1983) first demonstrated that the projected rotational velocities of horizontal branch stars in globular clusters, having values of $v\sin i$ up to 30 km s^{-1} , are significantly higher than in their field counterparts, and speculation has long existed that the ubiquitous chemical abundance anomalies in globular clusters (which in many cases appear to have a bimodal signature) and which are absent among halo field stars, are also driven by different angular momentum profiles (Norris 1981; Suntzeff 1981). While no satisfactory model currently exists to explain the rich and somewhat bewildering literature on globular cluster abundance variations (now known to involve C, N, O, Mg, Na, Al, Ba, and Eu (see Sneden et al. 1997, and references therein⁹)),

⁹For simplicity we exclude from discussion the even more complicated abundance patterns

the signatures of abundance variations have been found even at or near the main sequence turnoffs of some clusters (eg. 47 Tuc (Briley et al. 1996), NGC 6752 (Suntzeff & Smith 1991), and, most importantly in this context, M92 (King et al. 1998)). In M92, King et al. report ranges in the abundances of Mg, Na, and Ba in the same stars for which Li variations have been found, though they were unable to discern any systematic correlation between the behavior of Li, on the one hand, and the heavier elements, on the other.

While most efforts to understand the abundance anomalies have centered on the angular momentum distribution within individual stars, under the supposition that internal rotation might drive mixing, this provides an inadequate explanation for the existence of variations at and below the main-sequence turnoff (Da Costa & Demarque 1982). Alternatively one might speculate on pre-main-sequence origins for the phenomenon, and interactions between crowded protostellar disks have been proposed by Kraft (1998) as a possible mechanism for generating different abundance patterns in cluster environments. In this context, then, is it possible that interactions between the disks in the dense cluster environment enforce a diversity of evolutionary paths for the stars' angular momenta, which then affect the Li profiles in these objects? As most of the Li depletion and dispersion in the rotationally-induced turbulent models occurs during the first < 0.3 Gyr (Pinsonneault et al. 1992, Fig. 7), it is possible that the crowded cluster environments are affected by interactions between protostellar disks at just this crucial, early phase, producing different initial conditions to those found in lower density star clusters which ultimately dissolved to form the field population. If the environmental conditions have given rise to different Li-processing histories and generated different $A(\text{Li})$ spreads, then we must re-ask whether the thinness of the field Li plateau signifies a lack of depletion or merely depletion under conditions that were similar from one field star to another.

of the cluster ω Centauri (Norris & Da Costa 1995).

Alternatively, the $A(\text{Li})$ spread in M92 may be due to some other unidentified cause, which may possibly also explain the high abundance in the field star BD+23°3912 (King, Deliyannis, & Boesgaard 1996). In the field population, such enigmatic stars appear to be even less common than the ultra-Li-depleted stars, so it may be appropriate to regard them (or “it”) as rare pathological cases not requiring us to lose sight of the “health” of the majority of Li plateau stars. Purists may argue, with some merit, that the Population II lithium origin cannot be determined with certainty until all such exceptions are understood. The observations in M92 raise the interesting possibility that globular cluster stars may exhibit quite different Li processing histories than the field stars. We stand to learn more not only about Li but also about the differences in globular cluster and low density cluster environments from more detailed study, at higher S/N, of additional stars in this and other globular clusters.

8. Concluding Remarks

The vast majority (91%) of our very metal-poor, main-sequence turnoff, field sample is consistent with an observed scatter of only

$$\sigma_{\text{obs}} = 0.031 \text{ dex}$$

about a mean $A(\text{Li}) = 2.11$ dex. G186-26, being ultra-Li-depleted, was rejected (ab initio) from the analysis; it is a reminder that some stars deplete their Li by 1 dex or more. BD+9°2190 was rejected by the outlier-detection algorithm from the “best” sample on account of an anomalous abundance compared to the other stars. Even so, the larger formal errors associated with this star make it unclear whether it is genuinely depleted, or merely an inferior observation. Its inclusion in the “best” sample would have inflated the observed scatter to only 0.037 dex, compared to the expected errors $\sigma_{\text{err}} = 0.033$ dex, so irrespective

of its status we conclude that the intrinsic scatter of $A(\text{Li})$ for the metal-poor turnoff is

$$\sigma_{\text{int}} < 0.02 \text{ dex.}$$

We have again found a strong dependence of $A(\text{Li})$ on metallicity,

$$dA(\text{Li})/d[\text{Fe}/\text{H}] = 0.118 \pm 0.023 \text{ dex per dex,}$$

which is concordant with theoretical GCE models and with observed ${}^6\text{Li}$ levels.

Four systematic uncertainties are discussed. Three involve the adopted temperature scale, the atmospheric models, and interpretation of the GCE contamination revealed by ${}^6\text{Li}$ and the metallicity trend. These systematic uncertainties are $\simeq 0.10$ dex in each instance. In this study, the effective-temperature zeropoint was set by Magain's (1987) and Bell & Oke's (1986) $b - y$ calibrations of metal-poor stars, and the model atmospheres are from Bell (1983), which do not possess the convective overshoot used in Kurucz's (1993) models. The fourth systematic uncertainty surrounds possible stellar depletion of the pre-stellar Li. The inferred intrinsic scatter, if any, must be essentially zero, $\sigma_{\text{int}} < 0.02$. This is much less than the range expected for the rotationally-induced turbulent mixing mechanism of Pinsonneault et al. (1998), and we conclude that depletion by that mechanism must be < 0.1 dex. If essentially no surface Li has been destroyed in these very metal-poor turnoff stars, then the only substantial correction required to the mean abundance is for GCE, leading to a primordial abundance *lower* than the plateau mean. We infer $A(\text{Li})_p \simeq 2.00$ dex. The three surviving, potential systematic uncertainties listed at the beginning of this paragraph are $\simeq 0.10$ dex each.

The difference between our field star observations and the M92 data of Boesgaard et al. (1998) suggests that real field-to-cluster differences in Li evolution may have occurred. These may indicate different angular momentum evolutionary histories, possibly associated

with interactions between protostellar disks in the dense globular cluster environments. Further accurate study of Li in globular clusters will be required.

The authors gratefully acknowledge discussions with Dr C. P. Deliyannis and Dr J. A. Thorburn on an earlier, similar, proposal that was not supported by the telescope time assignment committees. They are grateful to Dr W. J. Schuster for supplying new Strömgren photometry ahead of publication, and to Dr A. Pedrosa for obtaining the WHT service observation. They also record their thanks to the Director and staff of the Anglo-Australian Observatory and the Australian Time Assignment Committee for the provision of facilities during this investigation. T.C.B. acknowledges partial support for this work from grants AST 90-1376, AST 92-22326, INT 94-17547, and AST 95-29454 awarded by the National Science Foundation.

REFERENCES

Akritas, M. G. & Bershady, M. A. 1996, *ApJ*, 470, 706

Alonso, A., Arribas, S., & Martinez-Roger, C. 1996a, *A&A*, 313, 873

Alonso, A., Arribas, S., & Martinez-Roger, C. 1996b, *A&AS*, 117, 227

Beers, T. C., Flynn, K., & Gebhardt, K. 1990 *AJ*, 100, 32

Beers, T. C., Preston, G. W., & Shectman, S. A. 1992, *AJ*, 103, 1987

Beers, T. C., Rossi, S., Norris, J. E., Ryan, S. G., Molaro, P., & Rebolo, R. 1998, *Space Science Reviews*, 84, 139

Beers, T. C., Rossi, S., Norris, J. E., Ryan, S. G., & Shefler, T. 1999, *AJ*, in press (Feb)

Bell, R. A. 1983, private communication

Bell, R. A., & Oke, J. B. 1986, *ApJ*, 307, 253

Bevington, P. R. 1969, *Data Reduction and Error Analysis for the Physical Sciences* (New York: McGraw-Hill)

Boesgaard, A. M. 1985, *PASP*, 97, 784

Boesgaard, A. M., Deliyannis, C. P., Stephens, A., & King, J. R. 1998, *ApJ*, 493, 206

Bonifacio, P. & Molaro, P. 1997, *MNRAS*, 285, 847

Bonifacio, P. & Molaro, P. 1998, *ApJ*, 500, L175

Briley, M.M., Smith, V.V., Suntzeff, N.B., Lambert, D.L., Bell, R.A., & Hesser, J.E. 1996, *Nature*, 383, 604

Burbidge, G. & Hoyle, F. 1998, *ApJ*, 509, L1

Burstein, D. & Heiles, C. 1982, *AJ*, 87, 1165

Carlsson, M., Rutten, R. J., Bruls, J. H. M. J., & Shchukina, N. G. 1994, *A&A*, 288, 860

Carney, B. W., Latham, D. W., Laird, J. B., & Aguilar, L. A. 1994, AJ, 107, 2240

Cayrel, R. 1988, The Impact of Very High S/N Spectroscopy on Stellar Physics, ed. G. Cayrel de Strobel & M. Spite, (Dordrecht: Kluwer), p345

Da Costa, G.S. & Demarque, P. 1982, ApJ, 259, 193

D'Antona, F. & Matteucci, F. 1991, A&A, 248, 62

Deliyannis, C. P. 1995, The Light Element Abundances, ed. P. Crane, (Berlin: Springer-Verlag), 395

Deliyannis, C. P., Boesgaard, A. M. & King, J. R. 1995, ApJ, 452, L13

Deliyannis, C. P., Demarque, P., & Kawaler, S. D. 1990, ApJS, 73, 21

Deliyannis, C. P. & Malaney, R. A. 1995, ApJ, 453, 810

Deliyannis, C. P., Pinsonneault, M. H. & Duncan, D. K. 1993, ApJ, 414, 740

Eggen, O. J. 1980, ApJS, 43, 457

Eggen, O. J. 1987, AJ, 93, 379

Fields, B. D. & Olive, K. A. 1998, preprint (astro-ph/9811183)

Gratton, R. G., Carretta, E., & Castelli, F. 1996, A&A, 314, 191

Hobbs, L. M. & Duncan, D. K. 1987, ApJ, 317, 796

Hobbs, L. M. & Pilachowski, C. 1988, ApJ, 326, L23

Hobbs, L. M., & Thorburn, J. A. 1991, ApJ, 375, 116

Hobbs, L. M., & Thorburn, J. A. 1994, ApJ, 428, L25

Hobbs, L. M., & Thorburn, J. A. 1997, ApJ, 491, 772

Hobbs, L. M., Welty, D. E., & Thorburn, J. A. 1991, ApJ, 373, L47

King, J. R., Deliyannis, C. P. & Boesgaard, A. M. 1996, AJ, 112, 2839

King, J. R., Stephens, A., Boesgaard, A. M., & Deliyannis, C. P. 1998, AJ, 115, 666

Kraft, R. P. 1998, private communication

Kurucz, R. L. 1993, CD-ROM 13: ATLAS9 Stellar Atmosphere Programs and 2 km/s grid, (Cambridge MA: SAO)

Lambert, D. L. 1995, A&A, 301, 478

Levine, D. M., Berenson, M. L., & Stephan, D. 1998, Statistics for Managers (Upper Saddle River: Prentice Hall), §5.6

Li, G. 1985, Exploring Data Tables, Trends, and Shapes, ed. D.C. Hoaglin, F. Mosteller, & J. W. Tukey (New York: Wiley), 281

Lucke, P. B. 1978, A&A, 64, 367

Magain, P. 1987, A&A, 181, 323

Molaro, P., Primas, F., & Bonifacio, P. 1995, A&A, 295, L47

Norris, J. 1981, ApJ, 248, 177

Norris, J. E. 1999, The Galactic Halo, ASP Conf. Ser., ed. B. K. Gibson, T. S. Axelrod, & M. E. Putman, (San Francisco: ASP), in press

Norris, J. E. & Da Costa, G. S. 1995, ApJ, 447, 680

Norris, J. E., Ryan, S. G., & Beers, T. C. 1997, ApJ, 488, 350

Norris, J. E., Ryan, S. G., Beers, T. C., & Deliyannis, C. P. 1997a, ApJ, 485, 370

Norris, J. E., Ryan, S. G., & Stringfellow, G. S. 1994, ApJ, 423, 386

Olive, K. A., & Schramm, D. N. 1992, Nature, 360, 439

Peterson, R.C. 1983, ApJ, 275, 737

Peterson, R.C., Tarbell, T.D., & Carney, B.W. 1983, ApJ, 265, 972

Pilachowski, C. A., Hobbs, L. M., & De Young, D. S. 1989, ApJ, 345, L39

Pinsonneault, M. H., Deliyannis, C. P., & Demarque, P. 1992, *ApJS*, 78, 179

Pinsonneault, M. H., Walker, T. P., Steigman, G., & Narayanan, V. K. 1998, preprint
(astro-ph/9803073)

Prantzos, N., Casse, M., & Vangioni-Flam, E. 1993, *ApJ*, 403, 630

Ramaty, R., Kozlovsky, B., & Lingenfelter, R. E. 1996, *ApJ*, 456, 525

Ramaty, R., Kozlovsky, B., Lingenfelter, R. E. & Reeves, H. 1997, *ApJ*, 488, 730

Rebolo, R., Molaro, P. & Beckman, J. E. 1988, *A&A*, 192, 192

Rousseeuw, P.J. & Leroy, A.M. 1987, Robust Regression and Outlier Detection (New York: Wiley)

Ryan, S. G. 1989, *AJ*, 98, 1693

Ryan, S. G. 1995, “The Light Element Abundances”, ed. P. Crane, (Berlin: Springer-Verlag), 276

Ryan, S. G. 1996, Formation of the Galactic Halo — Inside and Out (ASP Conf.Ser. 92), ed. H. Morrison & A. Sarajedini, (San Francisco: ASP), 113

Ryan, S. G., Beers, T. C., Deliyannis, C. P., & Thorburn, J. A. 1996a, *ApJ*, 458, 543

Ryan, S. G. & Norris, J. E. 1991, *AJ*, 101, 1835

Ryan, S. G., Norris, J. E., & Bessell, M. S. 1991, *AJ*, 102, 303

Ryan, S. G., Norris, J. E., & Beers, T. C. 1996b, *ApJ*, 471, 254

Ryan, S. G., Norris, J. E., & Beers, T. C. 1998, *ApJ*, 506, 892

Sandage, A. & Fouts, G. 1987, *AJ*, 93, 74

Sandage, A. & Kowal, C. 1986, *AJ*, 91, 1140

Savage, B. D. & Mathis, J. S. 1979, *ARA&A*, 17, 73

Schuster, W. J. 1998, private communication

Schuster, W. J. & Nissen, P. E. 1988, A&AS, 73, 225

Schuster, W. J. & Nissen, P. E. 1989, A&A, 222, 65

Schuster, W. J., Nissen, P. E., Parrao, L., Beers, T. C., & Overgaard, L. P. 1996, A&AS, 117, 317

Schuster, W. J., Parrao, L., & Contreras Martinez, M. E. 1993, A&AS, 97, 951

Searle, L. & Zinn, R. 1978, ApJ, 225, 357

Smith, V. V., Lambert, D. L., & Nissen, P. E. 1993, ApJ, 408, 262

Smith, V. V., Lambert, D. L., & Nissen, P. E. 1998, ApJ, 506, 405

Sneden, C., Kraft, R. P., Shetrone, M. D., Smith, G. H., Langer, G. E., & Prosser, C. F. 1997, AJ, 114, 1964

Spite, F. & Spite, M. 1982, A&A, 115, 357

Spite, F. & Spite, M. 1986, A&A, 163, 140

Spite, F. & Spite, M. 1993, A&A, 279, L9

Spite, M., François, P., Nissen, P. E., & Spite, F. 1996, A&A, 307, 172

Spite, M., Maillard, J. P. & Spite, F. 1984, A&A, 141, 56

Spite, M., Spite, F., Peterson, R. C. & Chaffee, F. H. Jr 1987, A&A, 172, L9

Steigman, G., & Walker, T. P. 1992, ApJ, 385, L13

Suntzeff, N. B. 1981, ApJS, 47, 1

Suntzeff, N. B. & Smith, V. V. 1991, ApJ, 381, 160

Thorburn, J. A. 1994, ApJ, 421, 318

Thorburn, J. A. & Beers, T. C. 1993, ApJ, 404, L13

Vauclair, S. 1999, preprint (astro-ph/9902144)

Vauclair, S. & Charbonnel, C. 1995, A&A, 295, 715

Yoshii, Y., Kajino, T., & Ryan, S. G. 1997, ApJ, 485, 605

Figure captions

Fig. 1: Spectra in region of the Li 6707 Å line, offset by multiples of 0.1 continuum units. Multiple epochs have been co-added for this illustration, and the continuum location has been indicated with a dotted line, but actual measurements of equivalent widths were made for each epoch separately, to check repeatability. See text for details.

Fig. 2: Comparison of equivalent width measurements for stars in common to our work and the accurate isotope ratio work of Smith et al. (1998). Our data are in agreement with theirs within $\pm 1.8\sigma$ at worst, and considerably better in many cases. The *dotted line* is the 1:1 locus.

Fig. 3: Dereddened Strömgren c_1^0 vs $(b - y)_0$ diagram showing our turnoff sample (*solid symbols*) against the general halo sample with $[\text{Fe}/\text{H}] < -1.0$ of Schuster, Parrao, & Contreras Martinez (1993) (*crosses*).

Fig. 4: Dereddened indices available to measure effective temperature, as a function of $(b - y)_0$. (a) The solid line coinciding with the data is from the theoretical colors of Bell & Oke (1986) for $[\text{Fe}/\text{H}] = -2$ and $\lg g = 4.0$. The solid line sitting away from the data is the transformation of Magain (1987) at $[\text{Fe}/\text{H}] = -2.8$. (b) and (c) *Solid lines*: Bell & Oke theoretical colors. (d) and (e) *Solid lines*: least squares fits of $(b - y)_0$ to the index, used to predict $(b - y)_0$ from the measured indices.

Fig. 5: Metallicity sensitivity of color-effective temperature calibrations for metal-poor turnoff stars: *solid curve*: synthetic colors of Kurucz (1993); *dashed curve* ((a) and (d) only): empirical fit to IRFM temperatures by Magain (1987); *dotted curve*: empirical fit to IRFM temperatures by Alonso et al. (1996a). Pairs of values are traced for each color. In the Kurucz and Magain calibrations, the sensitivity to metallicity decreases as expected as $[\text{Fe}/\text{H}]$ falls from -1 , whereas the Alonso et al. calibrations go through a minimum before

increasing non-physically towards yet lower metallicity. (a) $B-V = 0.35$ and 0.40 . The *solid bar* shows the metallicity range of our sample. (b) $(V-R)_C = 0.26$ and 0.28 (which were transformed to Johnson colors for Alonso et al’s calibration). (c) $(R-I)_C = 0.29$ and 0.31 (which were transformed to Johnson colors for Alonso et al’s calibration). (d) $b-y = 0.29$ and 0.32 . Alonso et al’s calibration appears highly non-physical over the range $[Fe/H] < -1$. Their $b-y = 0.29$ curve is shown for two values of $c_1 = 0.32$ and 0.38 ; the lower curve is for $c_1 = 0.30$. (e) $\beta = 2.60$ and 2.62 for Alonso et al. calibration, and $\beta = 2.65$ and 2.66 for Kurucz calibration.

Fig. 6: (a) Equivalent widths vs effective temperature. (b) Equivalent widths on lg scale, which is linear in $A(\text{Li})$. Solid line is for $A(\text{Li}) = 2.11$. (c) Spread in $A(\text{Li})$ about the 2.11 dex locus. Dashed lines are at ± 0.072 dex (2 s.d.) from the mean of the majority. (d) Histogram (upper) and stripe plot (lower) of $A(\text{Li})$ spread. The sample is seen to consist of a well defined bell curve to which the majority of the data conform, plus two stars lower in $A(\text{Li})$ by ~ 0.14 dex. See text for discussion.

Fig. 7: Spread in standardised residuals ($Z_i = (A_i(\text{Li}) - 2.11)/\sigma_{A(\text{Li}),i}$) about the 2.11 dex locus. See text for discussion.

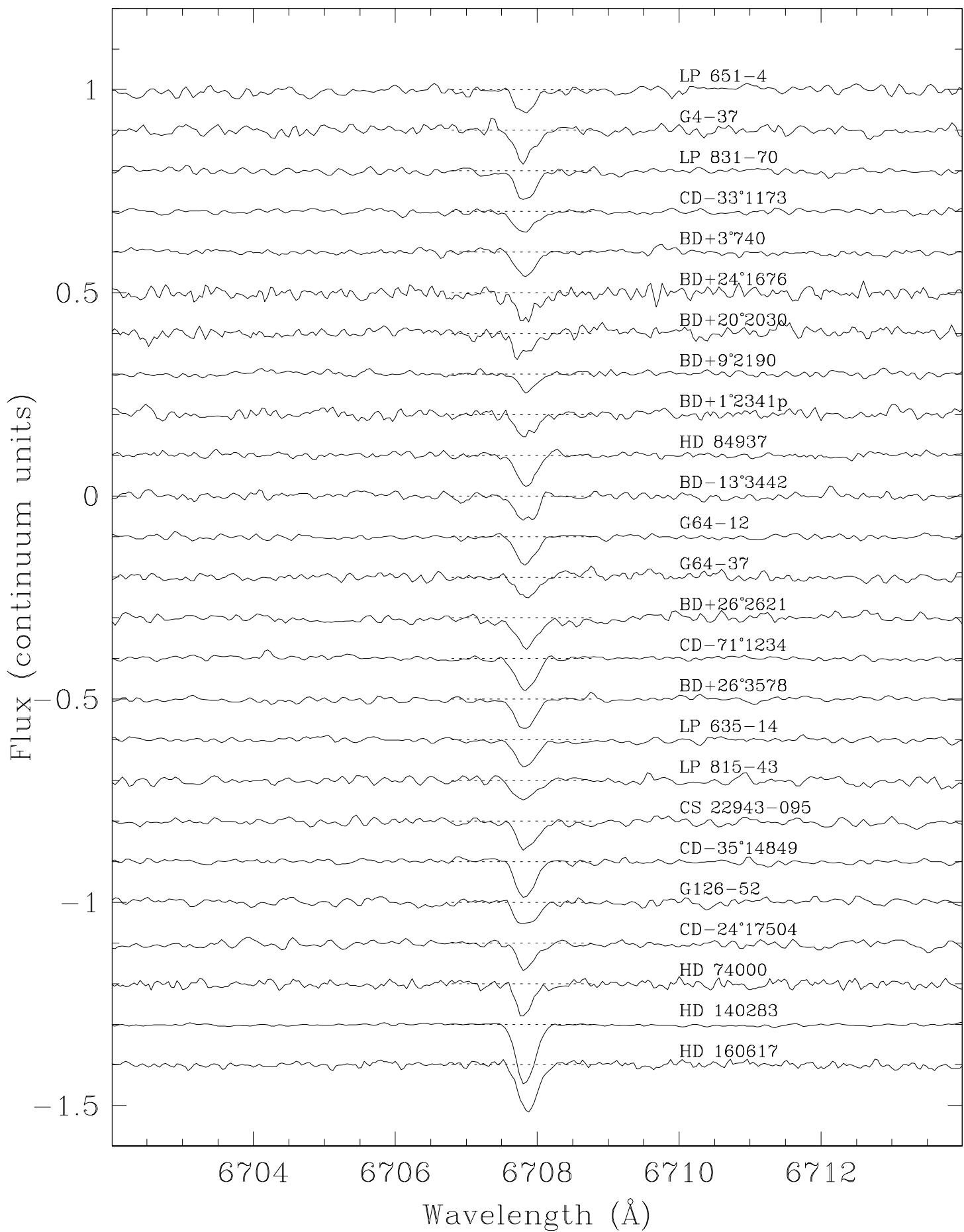
Fig. 8: (a-d) “Best Fit” sample (G186-26 rejected a priori). (a) Dependence of $A(\text{Li})$ on $[Fe/H]$. *Dotted line*: Univariate OLS fit for all stars; *solid line*: Univariate RWLS fit in which BD+9°2190 was rejected by the analysis as an outlier. This is our “best fit” regression. (b) $A(\text{Li})$ residuals from best fit. (c) Distribution of residuals shown as both a conventional histogram and a stripe plot. (d) “Normal probability plot” confirming that the residuals are distributed normally (see text). *Dotted line*: OLS fit to guide the eye, to highlight linearity. (e-h) “Culled Fit” sample from which BD+9°2190, CD-24°17504 and CD-71°1234 have been excluded, illustrating that even a culled sample yields a significant metallicity dependence. (e) Dependence of $A(\text{Li})$ on $[Fe/H]$. *Solid line*: Univariate RWLS

fit in which BD+9°2190 was excluded a priori, and subsequently CD–24°17504 and CD–71°1234 were rejected by the analysis as outliers. (f) As for (b). (g) As for (c). (h) As for (d).

Fig. 9: (a-d) Lithium abundances derived for two sets of effective temperature values, and plotted against two sets of [Fe/H] values; *solid line* = OLS fit. (e-f) Metallicities derived from 1Å-resolution spectra compare well with the high-resolution values adopted in this study, but unfavourably with several values adopted by Bonifacio & Molaro (1997). *Dotted line* = 1:1 locus for different [Fe/H] scales.

Due to the large scatter introduced by the IRFM temperatures and the disagreement between the [Fe/H] values from 1Å-resolution spectra and the values adopted by Bonifacio & Molaro, we argue that panel (a) is the most reliable presentation of the data. See text for discussion.

Fig. 10: (a) Depletion curves from Pinsonneault et al. (1998) “s0” model, broadened for formal errors of 0.033 dex. *Solid curve*: median depletion; *dashed curves*: boundaries enclosing $\pm 47.5\%$ of the population. The observational data have been superimposed for an assumed initial $A(\text{Li})_i = 2.23$. (b) *Shaded histogram*: “s0” model renormalized to our sample size, assuming $A(\text{Li})_i = 2.23$; *heavy histogram*: observations uncorrected for embedded metallicity dependence. (c) *Shaded histogram*: “s0” model as for (b); *heavy histogram*: observations offset to $[\text{Fe}/\text{H}] = -2.8$ to compensate for the embedded metallicity dependence. The model predicts a Li-depleted tail comprising 17% of the sample, but it is not populated by the observations.



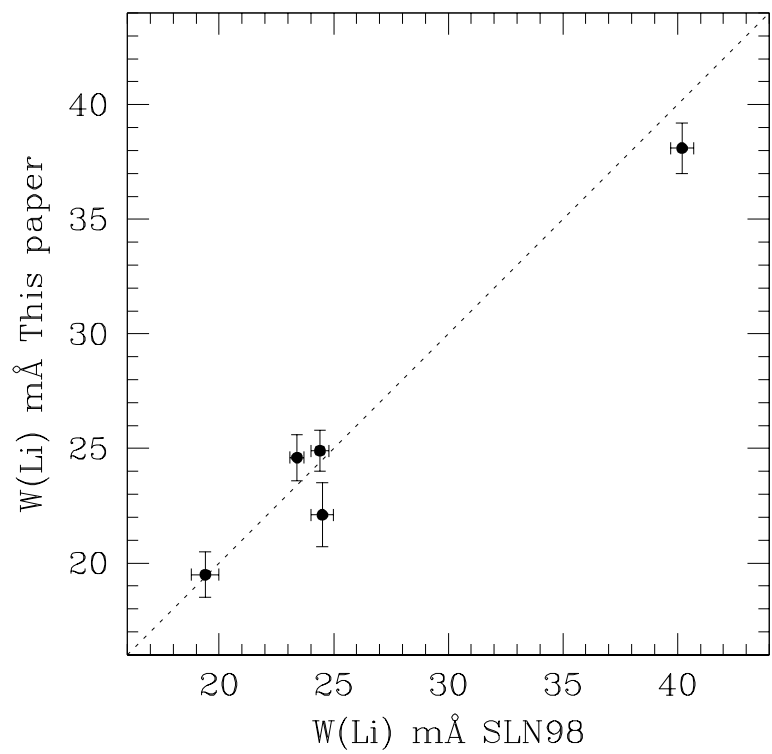


TABLE 2
LITHIUM EQUIVALENT WIDTHS FOR PROGRAM STARS

Star	[Fe/H] lit.	Refs	[Fe/H] 1 Å	T_{eff} K	σ_T K	S/N per 0.05 Å pixel				W mÅ			σ_W mÅ	
						96	97	98A	98B	96	97	98A	98B	
LP 651-4	-2.96	1	-2.60	6240	30	60	90		65	26.0	16.9	19.3	3.4	2.3
G4-37	-2.73	1,2	-2.70	6050	40		90				25.9			2.3
LP 831-70	-3.25	3	-3.32	6050	20		105		100		20.7			2.0
CD-33°1173	-3.14	3	-2.91	6250	20		115		130		18.5			1.6
BD+3°740	-2.78	2	-2.70	6240	40			130	130			20.0	18.9	1.6
BD+24°1676	-2.71	2	-2.38	6170	30			95				21.1		2.2
BD+20°2030	-2.71	2	-2.64	6200	40			105				21.4		2.0
BD+9°2190	-2.89	1,2	-2.83	6250	30			85	115 ^a			12.2	15.9 ^a	2.4
BD+1°2341p	-2.82	1,2	-2.79	6260	40			130				17.8		1.6
HD 84937	-2.30	1,2	-2.12	6160	30			195				24.9		1.1
BD-13°3442	-2.99	3	-2.79	6210	30			110	100			21.5	20.4	1.9
G64-12	-3.17	3	-3.24	6220	30		150		115		22.4		19.2	1.4
G64-37	-3.23	3	-3.15	6240	30		90	100			19.5	17.2		2.3
BD+26°2621	-2.88	2		6150	40			140					22.5	1.5
CD-71°1234	-2.50	3	-2.60	6190	30		140	110	125		25.6	26.8	25.5	1.5
BD+26°3578	-2.54	2	-2.24	6150	40		185				24.6			1.1
G186-26	-2.85	2	-2.62	6180	40									
LP 635-14	-2.65	3	-2.66	6270	30		135		115		19.1		21.8	1.5
LP 815-43	-3.05	3	-3.00	6340	30	85	95			14.0	17.8		2.4	2.2
CS 22943-095	-2.55	4	-2.20	6140	40	95	75		110	20.1	26.8		23.5	2.2
CD-35°14849	-2.63	1	-2.38	6060	20		145				28.8			1.4
G126-52	-2.57	2	-2.45	6210	40		130				19.1			1.6
CD-24°17504	-3.55	3	-3.24	6070	20	85	90		95	19.2	15.1		19.9	2.4
<i>Standard stars:</i>														
HD 74000	-2.02	2		6040	30			130				22.1		1.6
HD 140283	-2.60						300		250		47.7		48.2	0.7
HD 160617									165			38.1		1.2
														0.8

^aWHT service observation from November 6, 1998.

REFERENCES.— (1) Ryan & Norris (1991), (2) Carney et al. (1994), (3) Ryan, Norris & Bessell (1991) adjusted to $A(\text{Fe})_{\odot} = 7.50$, (4) Beers, P.

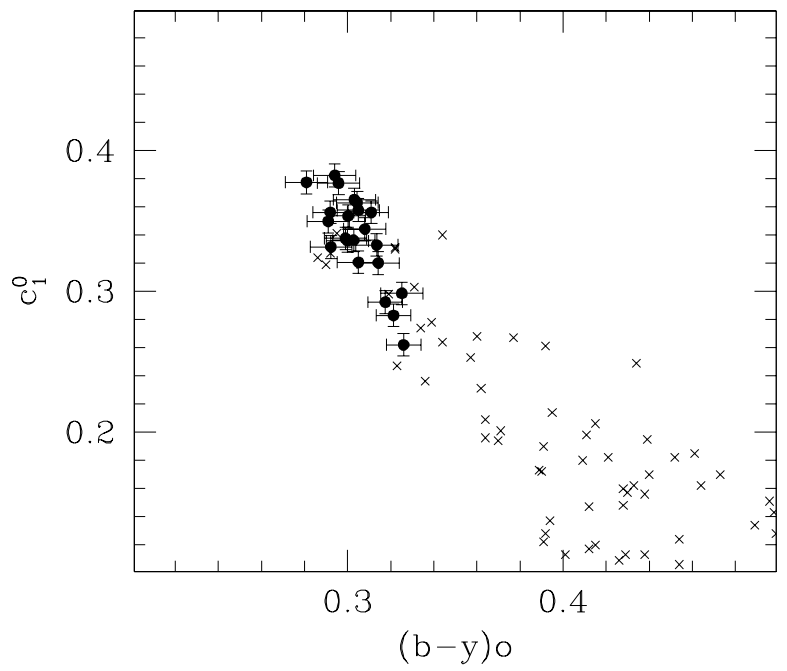


TABLE 3
EXTERNAL COMPARISON WITH LITERATURE DATA

Star	W _{Li}	σ_W	Refs
LP 651-4	19.6	1.6	RNB99
G4-37	25.9	2.3	RNB99
"	20	2.8	HT91
"	19	3.4	T94
LP 831-70	23.1	1.4	RNB99
"	26	2.1	SS93
"	23	2.6	T94
CD-33° 1173	17.2	1.2	RNB99
"	17	2.7	SS93
"	12	2.4	T94
"	10	1.5	NRS94
BD+03° 740	19.5	1.1	RNB99
"	17	1.5	HP88
"	21	4.8	RMB88
"	21	3.7	TB93
"	19.3	1.0	HT94
"	24	2.4	T94
"	23	1.0	RBDT96
"	25.0	4.5	SFNS93
"	19.4	0.6	SLN98
BD+24° 1676	21.1	2.2	RNB99
"	26	2.2	HT91
"	28	2.9	T94
BD+20° 2030	20.5	2.0	RNB99
"	23	2.2	T94
BD+09° 2190	14.7	1.3	RNB99
"	18	3.4	T94
"	20	1.5	RBDT96
BD+1° 2341p	17.8	1.6	RNB99
"	23	4.5	HD87
"	21	2.6	T94
HD 84937	24.9	1.1	RNB99
"	18	2.2	SS82
"	23	1.0	B85
"	20	3.0	HD87
"	25	1.0	PHD89
"	24.5	1.0	HT94
"	22	2.5	T94
"	25	1.0	RBDT96
"	26.2	1.0	RBDT96
"	25.0		SLN93
"	24.4	0.4	SLN98
BD-13° 3442	21.0	1.4	RNB99
"	30	3.4	T94
"	19	1.0	RBDT96
G64-12	21.2	1.1	RNB99
"	25	5.0	SSPC87
"	23	5	RBM87
"	31	4?	SS93
"	28	3.5	TB93
"	28	3.6	T94
G64-37	18.2	1.5	RNB99
"	14	1.6	T94
"	14	2.0	NRS94
"	16	1.5	RBDT96
"	18.0	4.5	SFNS96
BD+26° 2621	22.5	1.5	RNB99
"	20	2.9	T94

TABLE 3—*Continued*

Star	W _{Li}	σ_W	Refs
CD-71°1234	25.9	0.9	RNB99
"	27	2.9	T94
BD+26°3578	24.6	1.1	RNB99
"	24	1.7	SMS84
"	24	1.5	HD87
"	22.2	1.0	HT94
"	23.4	0.3	SLN98
LP 635-14	20.2	1.2	RNB99
"	24	3.9	T94
LP 815-43	16.1	1.6	RNB99
"	27	2.2	SS93
"	22	2.1	T94
"	15	3.2	NRS94
"	13	1.6	NRS94
CS 22943-095	23.0	1.3	RNB99
-35°14849	28.8	1.4	RNB99
"	30.8	5	SFNS96
G126-52	19.1	1.6	RNB99
"	26	3.6	T94
CD-24°17504	18.1	1.3	RNB99
"	22	4.1	SS93
"	21	3.4	T94
"	19	2.3	NRS94
HD 74000	22.1	1.6	RNB99
"	25	3.4	SS86
"	24.5	0.9	HT97
"	24.5	0.5	SLN98
HD 140283	47.9	0.5	RNB99
"	50		RMB88
"	46	1.8	T94
"	48	0.8	NRS94
"	46	3	SFNS96
HD 160617	38.1	1.2	RNB99
"	43.0	3	SFNS96
"	40.2	0.5	SLN98

REFERENCES.— SS82 = Spite & Spite 1982; SMS84 = Spite, Maillard, & Spite 1984; B85 = Boesgaard 1985; SS86 = Spite & Spite 1986; SSPC87 = Spite et al. 1987; HD87 = Hobbs & Duncan 1987; HP88 = Hobbs & Pilachowski 1988; RMB88 = Rebolo, Molaro & Beckman 1988; PHD89 = Pilachowski, Hobbs, & De Young 1989; HT91 = Hobbs & Thorburn 1991; SS93 = Spite & Spite 1993; TB93 = Thorburn & Beers 1993; HT94 = Hobbs & Thorburn 1994; T94 = Thorburn 1994; NRS94 = Norris, Ryan & Stringfellow 1994; RBDT96 = Ryan et al. 1996a; SLN93 = Smith, Lambert & Nissen 1993; SFNS96 = Spite et al. 1996; HT97 = Hobbs & Thorburn 1997; SLN98 = Smith, Lambert & Nissen 1998; RNB99 = this work.

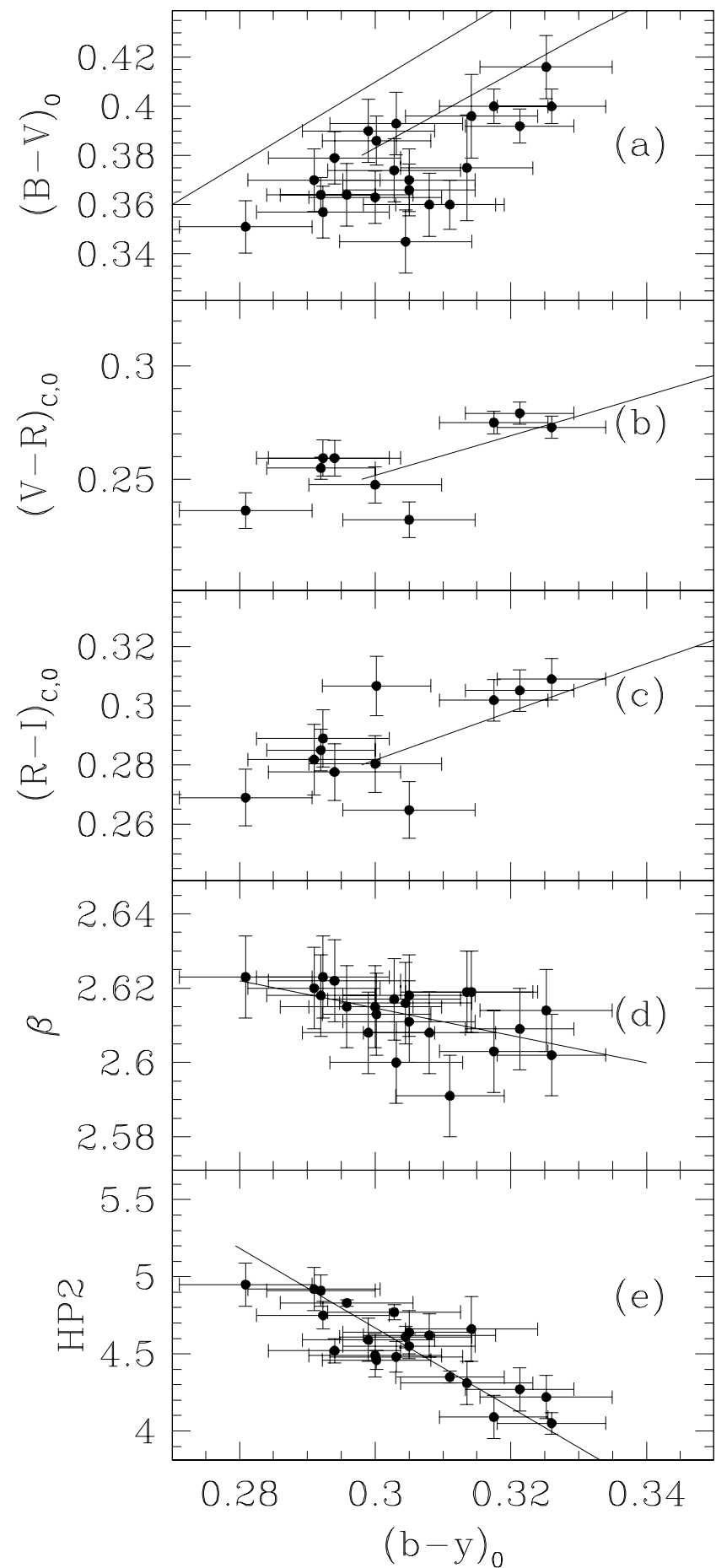


TABLE 4
HELIOCENTRIC RADIAL VELOCITIES FOR PROGRAM STARS

Star	v_{rad} km s^{-1}	Ref	Notes
LP 651-4	12.6 12.2 12.3	96 97 98B	
G4-37	-108.5 -108.5	CLLA94 97	1.0, 41, 3633
LP 831-70	-48.1 -48.4	97 98B	
CD-33° 1173	47.4 47.0	97 98B	
BD+3° 740	173.8 173.7 173.7	CLLA94 98A 98B	0.9, 14, 1809
BD+24° 1676	-238.4 -238.0	CLLA94 98A	1.0, 17, 2210
BD+20° 2030	-67.2 -55.9	CLLA94 98A	0.9, 34, 382, SB1
BD+9° 2190	266.1 266.1 265.8	CLLA94 98A WHT98	1.5, 38, 2839
G48-29	-57.4 -57.2	CLLA94 98A	1.6, 31, 2952
HD 84937	-14.8 -15.0	CLLA94 98A	0.9, 35, 3572
BD-13° 3442	115.8 115.2	98A 98B	
G64-12	441.9 441.8 442.2	CLLA94 97 98B	1.7, 24, 4406
G64-37	81.2 80.7 81.6	CLLA94 97 98A	1.4, 18, 1234
G166-54	-62.9 -62.9	CLLA94 98B	1.2, 18, 1508
CD-71° 1234	231.0 220.9 215.0	97 98A 98B	New SB1
BD+26° 3578	-129.1 -129.4	CLLA94 97	0.7, 17, 3072
LP 635-14	-117.9 -117.0	97 98B	
LP 815-43	-4.1 -4.2	96 97	
CS 22943-095	-150.1 -150.7 -150.5	96 97 98B	
CD-35° 14849	108.0	97	
G126-52	-242.1 -241.4	CLLA94 97	1.2, 21, 1799
BD-24° 17504	135.8 135.7 135.5	96 97 98B	
<i>Standard stars:</i>			
HD 74000	206.3 205.9	CLLA94 98A	0.9, 41, 3299
HD 140283	-170.9 -171.1 -170.4	CLLA94 97 98B	0.8, 19, 3115
HD 160617	99.4	98A	

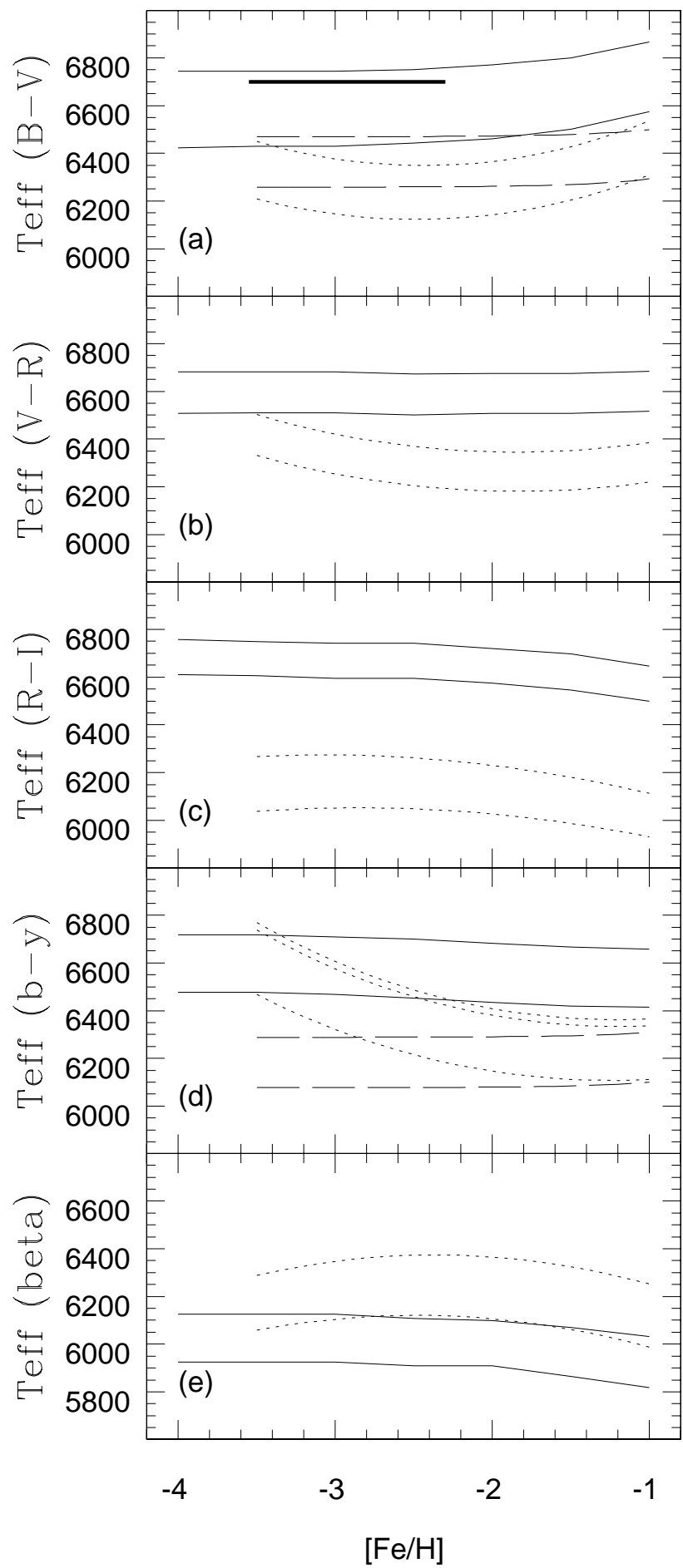


TABLE 5
RESULTS OF REGRESSION ANALYSES

Sample Size Initial ^a	Method	Fit	R ²	Notes
Initial Final				
Bivariate analyses				
22	= OLS	$A(\text{Li}) = 2.461(\pm 0.695) + 0.121(\pm 0.029) \times [\text{Fe}/\text{H}] + 0.000(\pm 0.011) \times T_{\text{eff}}$	0.48	
22	21 ^b RWLS	$A(\text{Li}) = 2.102(\pm 0.575) + 0.118(\pm 0.024) \times [\text{Fe}/\text{H}] + 0.006(\pm 0.009) \times T_{\text{eff}}$	0.59	
Univariate analyses with full sample				
22	= OLS	$A(\text{Li}) = 2.449(\pm 0.081) + 0.121(\pm 0.028) \times [\text{Fe}/\text{H}]$	0.48	dotted line, Fig. 8(a)
22	21 ^b RWLS	$A(\text{Li}) = 2.447(\pm 0.066) + 0.118(\pm 0.023) \times [\text{Fe}/\text{H}]$	0.58	solid line, Fig. 8(a)
22	= BCES	$A(\text{Li}) = 2.570(\pm 0.094) + 0.164(\pm 0.032) \times [\text{Fe}/\text{H}]$		
22	= BCES Bootstrap	$A(\text{Li}) = 2.480(\pm 0.093) + 0.132(\pm 0.033) \times [\text{Fe}/\text{H}]$		
22	= Robust	$A(\text{Li}) = 2.430(\pm 0.084) + 0.113(\pm 0.030) \times [\text{Fe}/\text{H}]$	0.48	
Univariate analyses with culled sample, excluding BD+9°2190, CD-24°17504 and CD-71°1234				
21 ^c	19 RWLS	$A(\text{Li}) = 2.318(\pm 0.063) + 0.073(\pm 0.022) \times [\text{Fe}/\text{H}]$	0.39	solid line, Fig. 8(e)
19	= OLS	^d		
19	= BCES	$A(\text{Li}) = 2.420(\pm 0.093) + 0.110(\pm 0.033) \times [\text{Fe}/\text{H}]$		
19	= BCES Bootstrap	$A(\text{Li}) = 2.350(\pm 0.081) + 0.083(\pm 0.028) \times [\text{Fe}/\text{H}]$		
19	= Robust	$A(\text{Li}) = 2.346(\pm 0.064) + 0.083(\pm 0.022) \times [\text{Fe}/\text{H}]$	0.39	

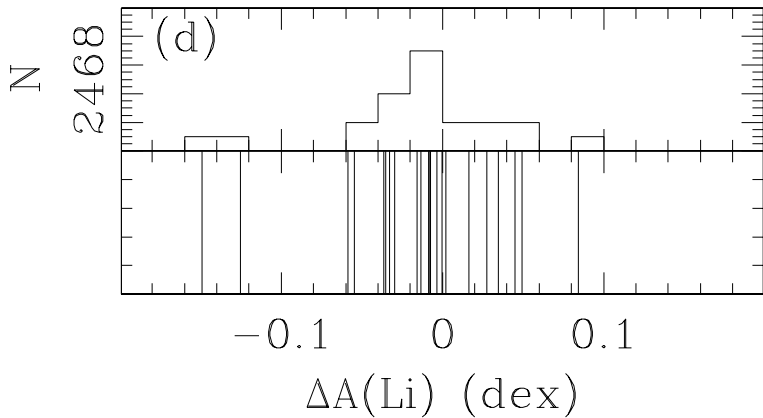
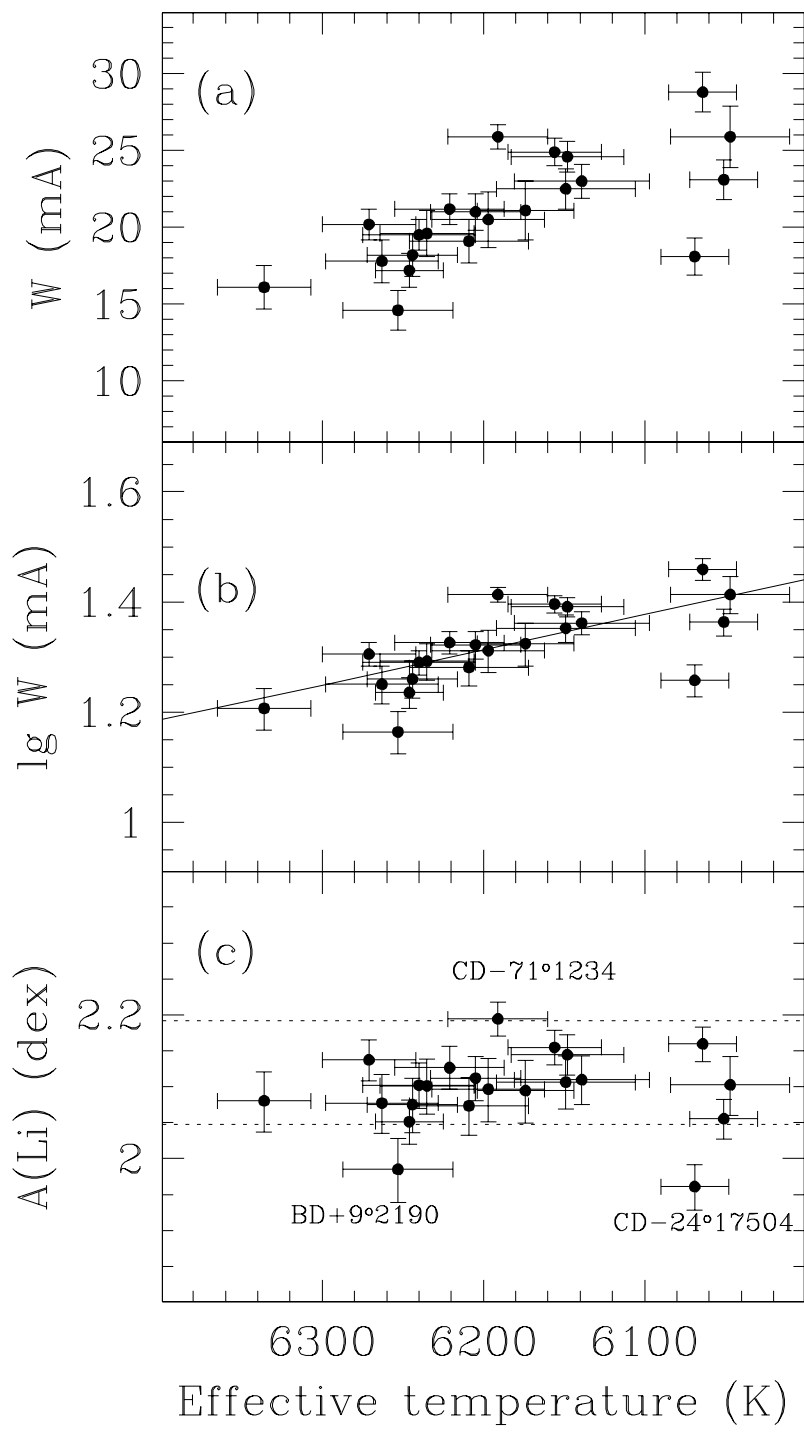
NOTE.—Stated errors are standard errors.

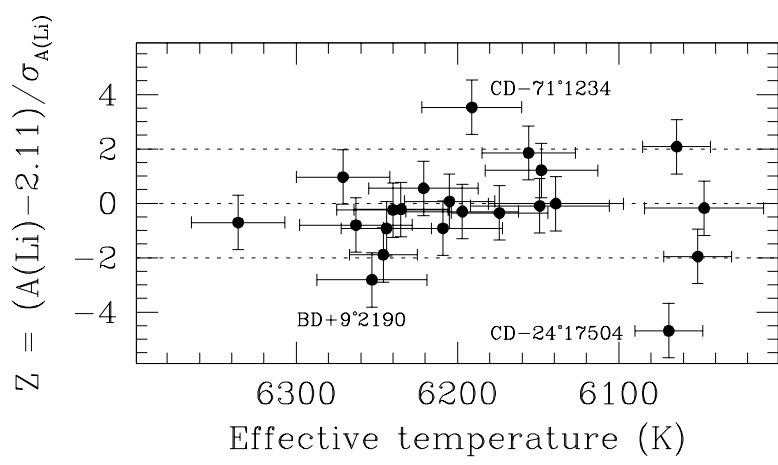
^aG186-26 was excluded from all analyses a priori.

^bBD+9°2190 was rejected by the analysis as an outlier.

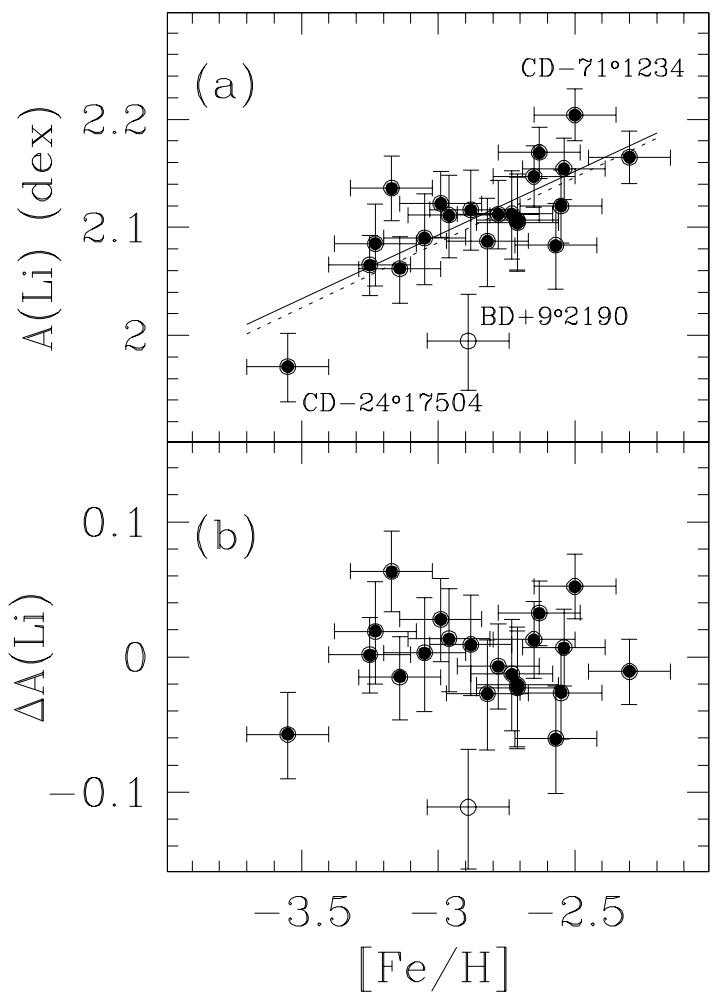
^cBD+9°2190 was excluded from this analysis a priori, and the other two stars were rejected by the analysis as outliers.

^dThis case is identical to RWLS with final sample=19.

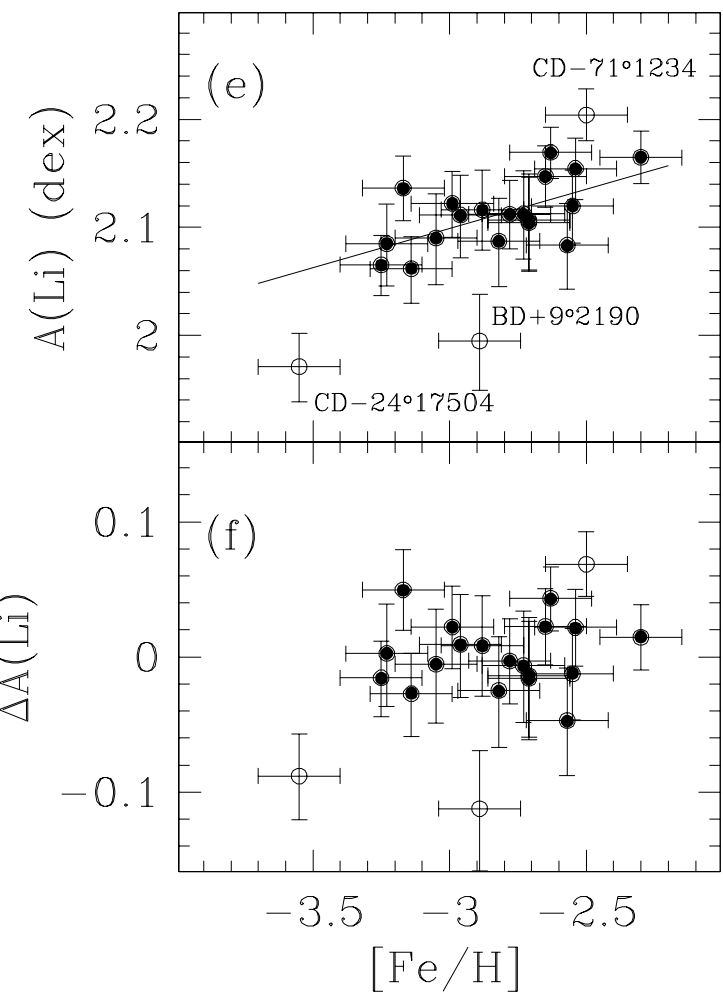


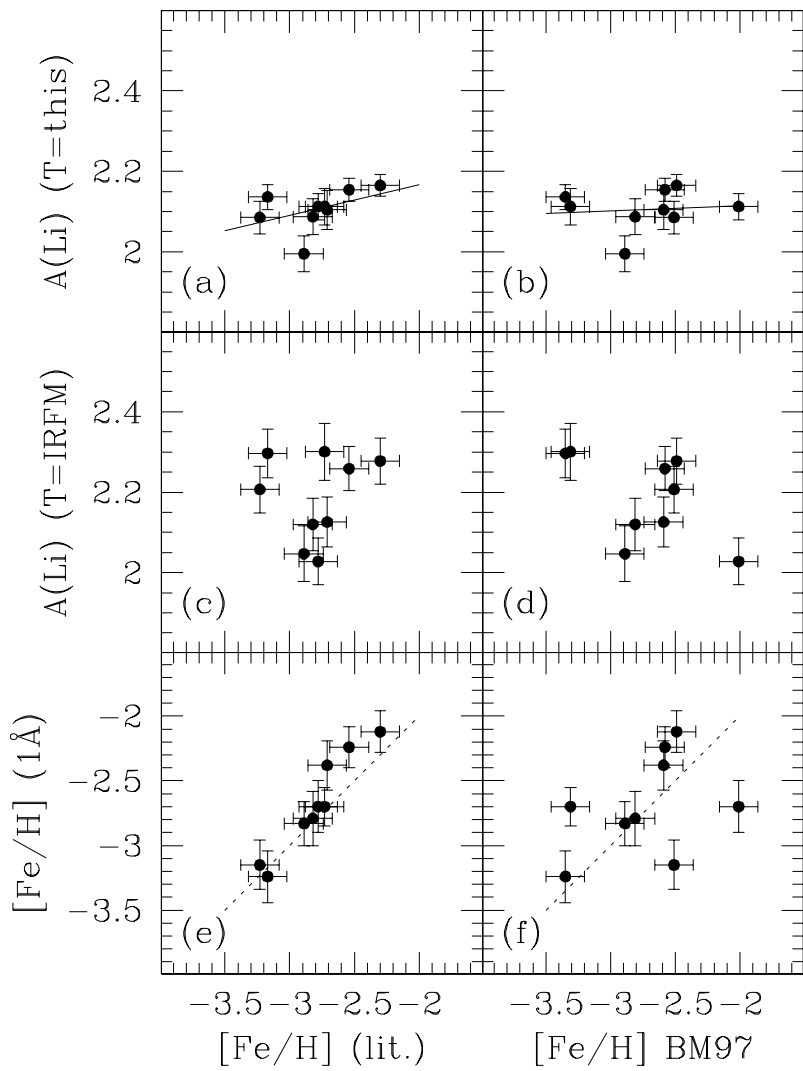


Best Fit



Culled Fit





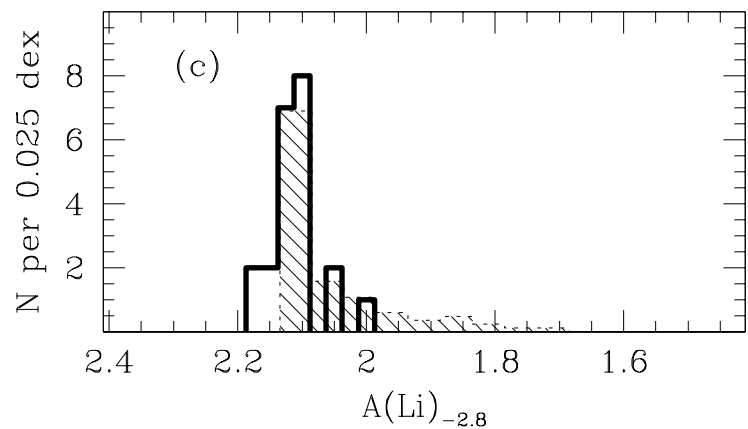
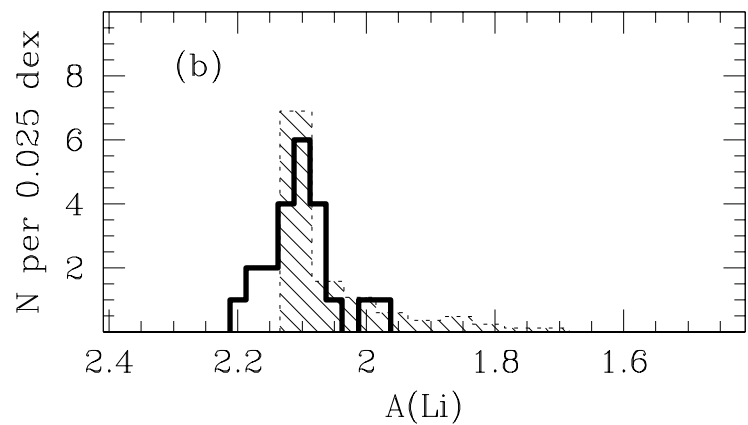
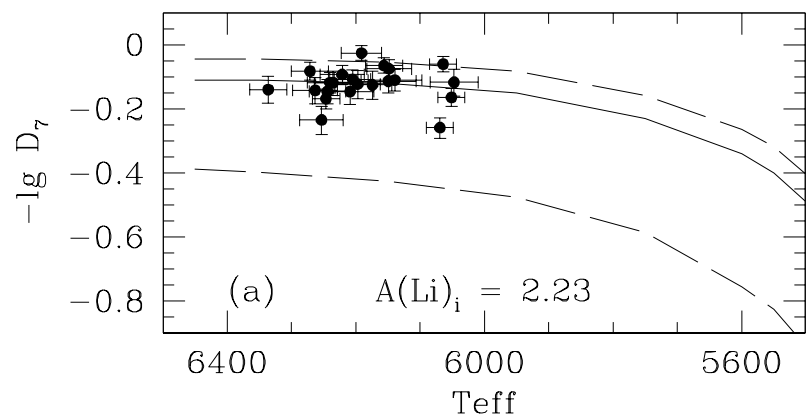


TABLE 1
PHOTOMETRY FOR PROGRAM STARS

Star		RA (1950)	Dec	V	B-V	V-R	R-I _c	E(BV)	n _J	b-y	c ₁	E(by)	n _S	β	n _β	I	
LP 651-4		024142	-053930	12.04	.393	.271	.305	.02	2	.321	.340	.043	4	2.615	4	5,12	
G4-37	Tou 23:443	024155	+081618	11.42	.47			.04	2	.363	.306	.063	6	2.614	7	1,6,7	
LP 831-70		030352	-223048	11.62	.400	.273	.309	.00	2	.326	.262	.014	4	2.602	4	5,12	
CD-33°1173		031734	-330124	10.94	.364	.255	.285	.00	2	.292	.356	.011	5	2.618	5	5,12	
BD+3°740	G84-29	045838	+040224	9.80	.36			.01	3	.315	.365	.028	5	2.616	5	1,6,7	
BD+24°1676	G88-32	072739	+241142	10.80	.36			.01	3	.311	.356	.000	3	2.591	3	1,6,7	
BD+20°2030	G40-14	081313	+195124	11.20	.38			.01	3	.312	.322	.021	6	2.618	6	1,6,12	
BD+9°2190	G41-41	092635	+085124	11.15	.38			.02	4	.307	.379	.023	5	2.615	5	1,6,7	
BD+1°2341p	G48-29	093808	+011436	10.47	.38		.29	.02	5	.298	.351	.014	9	2.620	6	1,3,6	
HD 84937	BD+14°2151	094617	+135918	8.33	.39		.31	.01	5	.303	.354	.013	9	2.613	8	1,2,6	
BD-13°3442		114418	-134954	10.26	.399	.275	.294	.01	2	.308	.385	.035	5	2.622	5	5,12	
G64-12	W 1492	133730	+001254	11.47	.38			.00	6	.307	.337	.023	7	2.617	8	1,6,7	
G64-37	R 841	135953	-052418	11.13	.368	.268	.298	.02	2	.300	.333	.015	10	2.623	10	1,5,6	
BD+26°2621	G166-54	145200	+254612	11.05	.41			.00	1	.324	.322	.034	11	2.619	13	1,12	
CD-71°1234		160218	-711400	10.44	.412	.277	.321	.04	2							5	
BD+26:3578	HD 338529	193029	+261706	9.35	.40			.02	2	.308	.366	.010	3	2.600	3	1,7,8	
G186-26		202237	+245330	10.82	.40			.02	2	.306	.339	.015	3	2.608	3	1,7,8	
LP 635-14		202413	-004700	11.33	.426	.279	.314	.05	2	.347	.366	.064	4	2.611	4	5,12	
LP 815-43		203521	-203630	10.91	.384	.262	.296	.04:	2	.304	.382	.033	4	2.623	4	5,12	
CS 22943-095		203559	-470052	11.76	.39:			.00		.324	.335	.036	3	2.619	3	4,9	
CD-35°14849	W 13543	213048	-353912	10.57	.405	.279	.306	.01	2	.321	.293	.014	4	2.603	2	5,7,8	
G126-52		220151	+191836	11.01	.38			.02	3	.322	.347	.028	3	2.608	3	1,6,12	
CD-24°17504	G275-4	230439	-240842	12.12	.393	.280	.306	.00	2	.322	.283	.015	5	2.609	5	5,12	
<i>Standard stars:</i>																	
HD 74000		083831	-160936	9.64	.42			.31	.00		.311	.295	-.01	7	2.596	4	1,3,7
HD 140283		154022	-104618	7.22	.49												
HD 160617																	

NOTE.— [Fe/H] is based on high and medium resolution spectra, in some instances weighted with photometric measurements; see referenced sources for details.

REFERENCES.— (1) Carney et al. (1994), (2) Eggen (1980), (3) Eggen (1987), (4) Beers, Preston & Shectman (1992), (5) Ryan (1989) (6) Sandage & Tammann (1981), (7) Schuster & Nissen (1989), (8) Schuster et al. (1996), (9) Schuster et al. (1993), (10) Schuster et al. (1993), (11) Sandage & Fouts (1987), (12) Schuster (1998).